

1 [Is it selfish to be filamentous in biofilms? Individual-based modeling](#)
2 [links microbial growth strategies with morphology using the new and](#)
3 [modular iDynoMiCS 2.0](#)

4 Running title: Individual-based modeling platform iDynoMiCS 2.0

5 Bastiaan J R Cockx^{1*}, Tim Foster², Robert J Clegg², Kieran Alden², Sankalp Arya³, Dov J Stekel³, Barth F
6 Smets¹, Jan-Ulrich Kreft^{2*}

7 ¹Department of Environmental and Resource Engineering, Technical University of Denmark,
8 Bygningstorvet, Bygning 115, 2800 Kgs. Lyngby, Denmark

9 ²Centre for Computational Biology & Institute of Microbiology and Infection & School of Biosciences,
10 University of Birmingham, Edgbaston, Birmingham, B15 2TT, UK

11 ³School of Biosciences, University of Nottingham, Sutton Bonington Campus, Loughborough,
12 Leicestershire, LE12 5RD, UK

13 ORCIDs

14 Bastiaan J R Cockx: 0000-0002-3751-0771

15 Tim Foster: 0000-0001-8559-0983

16 Robert J Clegg: 0000-0001-7041-9745

17 Kieran James Alden: 0000-0003-4411-1776

18 Sankalp Arya: 0000-0002-9081-1485

19 Dov J Stekel: 0000-0002-2492-8079

20 Barth F Smets: 0000-0003-4119-6292

21 Jan-Ulrich Kreft: 0000-0002-2351-224X

22 *Corresponding authors: Jan-Ulrich Kreft j.kreft@bham.ac.uk, Bastiaan J R Cockx: baco@dtu.dk

23 Abstract

24 Microbial communities are found in all habitable environments and often occur in assemblages with
25 self-organized spatial structures developing over time. This complexity can only be understood,
26 predicted, and managed by combining experiments with mathematical modeling. Individual-based
27 models are particularly suited if individual heterogeneity, local interactions, and adaptive behavior are
28 of interest. Here we present the completely overhauled software platform, the individual-based
29 Dynamics of Microbial Communities Simulator, iDynoMiCS 2.0, which enables researchers to specify a
30 range of different models without having to program. Key new features and improvements are: (1)
31 Substantially enhanced ease of use (graphical user interface, editor for model specification, unit
32 conversions, data analysis and visualization and more). (2) Increased performance and scalability
33 enabling simulations of up to 10 million agents in 3D biofilms. (3) Kinetics can be specified with any
34 arithmetic function. (4) Agent properties can be assembled from orthogonal modules for pick and mix
35 flexibility. (5) Force-based mechanical interaction framework enabling attractive forces and non-
36 spherical agent morphologies as an alternative to the shoving algorithm. The new iDynoMiCS 2.0 has
37 undergone intensive testing, from unit tests to a suite of increasingly complex numerical tests and the
38 standard Benchmark 3 based on nitrifying biofilms. A second test case was based on the “biofilms
39 promote altruism” study previously implemented in BacSim because competition outcomes are highly
40 sensitive to the developing spatial structures due to positive feedback between cooperative
41 individuals. We extended this case study by adding morphology to find that (i) filamentous bacteria
42 outcompete spherical bacteria regardless of growth strategy and (ii) non-cooperating filaments
43 outcompete cooperating filaments because filaments can escape the stronger competition between
44 themselves. In conclusion, the new substantially improved iDynoMiCS 2.0 joins a growing number of
45 platforms for individual-based modeling of microbial communities with specific advantages and
46 disadvantages that we discuss, giving users a wider choice.

47 Author summary

48 Microbes are fascinating in their own right and play a tremendously important role in ecosystems.
49 They often form complex, self-organized communities with spatial heterogeneity that is changing over
50 time. Such complexity is challenging to understand and manage without the help of mathematical
51 models. Individual-based models are one type of mathematical model that is particularly suited if
52 differences between individual microbes, local interactions and adaptive behavior are important. We
53 have developed a completely overhauled version of iDynoMiCS, a software that allows users to
54 develop, run and analyze a wide range of individual-based models without having to program the
55 software themselves. There are several capability enhancements and numerous small improvements,
56 for example the ability to model different shapes of cells combined with physically realistic mechanical
57 interactions between neighboring cells. We showcase this by simulating the competition between
58 filaments, long chains of cells, with single cells and find that filaments outcompete single cells as they
59 can spread quickly to new territory with higher levels of resources. Users now have a wider choice of
60 platforms so we provide guidance on which platform might be most suitable for a given purpose.

61 Introduction

62 Microbes are found everywhere on Earth where conditions are suitable for life, often as microbial
63 communities in self-organized assemblages such as biofilms [1]. They have a long evolutionary history
64 through which they diversified into a huge number of species with fascinating characteristics and
65 behaviors. Microbes master metabolism and thus enable biogeochemical cycles. Yet the complexity
66 arising from the high diversity of their communities undergoing spatio-temporal dynamics makes it
67 challenging to understand, predict and manage these communities [2]. This challenge can be best met
68 by an integration of *in situ* observations, experiments in mesocosms and laboratory models and
69 mathematical modeling [2].

70 Microbes growing in biofilms are a good example. Due to metabolic transformations of resources
71 diffusing into the self-assembling biofilms, the aggregates become spatially structured including
72 metabolite and resulting physiological gradients while growth leads to clonal populations. These
73 changing environmental conditions prompt differences in gene expression, phenotype and behavior
74 compared to planktonic cells [3]. For example, biofilm-dwelling *Pseudomonas aeruginosa* up-regulate
75 production of extracellular polysaccharides (EPS), while *Staphylococcus aureus* biofilms up-regulate
76 enzymes involved in glycolysis and fermentation [4]. Even in single species populations, phenotypic
77 heterogeneity can become substantial [5,6]. Coupled to the local environmental changes, biofilm
78 microbes experience selective pressures different to planktonic microbes. These are just a few points,
79 but they already demonstrate the challenge of complexity in biofilm communities.

80 Biofilms are also a good example of insights derived from mathematical modeling, going back to the
81 1970s [7]. Early models treated the biofilm as a continuum in one dimension (1D), which enabled
82 insights into substrate consumption driving the formation of gradients and diffusional fluxes and
83 vertical stratification [8–10]. A key insight from later 2D and 3D models enabling the emergence of
84 complex spatial structures was that the physics of mass transfer is sufficient to understand the
85 formation of finger-like biofilm structures, arising from a positive feedback in growth where the cells
86 at the surface of the biofilm with best access to substrate grow best so that their offspring are even
87 closer to the substrate source and grow even better [11–13]. The detailed reconstruction of early
88 biofilm growth observed through advanced microscopy coupled with detailed individual-based
89 modeling of mechanical cell-cell interactions demonstrated that mechanics alone is sufficient to
90 understand and predict early biofilm formation in *Vibrio cholerae* (before substrate gradients cause
91 growth limitations [14]).

92 In such individual-based models (IbMs), microbial cells are modeled as agents, partially autonomous
93 physical entities with individual properties and behavior [15]. This enables understanding of how these
94 individuals affect other individuals in the community and the environment and are affected by the
95 other individuals and the environment in turn. Properties of the community such as spatial patterns,
96 fitness, productivity and resilience emerge from the behavior of the individuals in that community.
97 IbMs are thus particularly suited to capture the effects of local interactions, individuality and
98 adaptative behavior on spatio-temporal dynamics. This includes stochastic events such as dispersal
99 and community assembly, up-regulation of genes, mutations or horizontal gene transfer. For example,
100 Hellweger [16] used an IbM to model the gene expression and differentiation of *Anabaena* spp.
101 individuals within a filament, and were able to reproduce almost all of the patterns observed *in vitro*.

102 To facilitate the use of individual-based modeling of microbial communities for scientists with little
103 experience of programming, the open source modeling platform iDynaMiCS (individual-based
104 Dynamics of Microbial Communities Simulator) was introduced [17], which we now refer to as
105 iDynaMiCS 1. It was the result of a collaborative effort merging features of previous models into a
106 common basis for further development. iDynaMiCS has been facilitating a range of studies and

107 influenced the design of other modeling platforms [18–23]. Here we present, after a long phase of
108 development and testing, a completely overhauled new version, simply called iDynaMiCS 2.0. We
109 came closer to the original aim of making iDynaMiCS easy to use for non-programmers while
110 substantially enhancing its capabilities and computational efficiency. Key new features and
111 improvements are: (1) Enhanced ease of use right from the start, from using a simple guided java
112 installer, lack of dependence on other software installations, a graphical user interface (GUI) for
113 running simulations, editing model specification (protocol) files, unit conversions, data analysis and
114 visualization of live results or re-loaded past results, a collection of model examples and online wiki for
115 guidance, autonomous adjustments for solver convergence. (2) Increased performance and scalability
116 enabling simulations of up to 10 million agents in 3D biofilms. (3) Kinetics of chemical or agent-
117 catalyzed reactions can now be specified with any user-chosen arithmetic function. Local or
118 intracellular conditions can be incorporated in these expressions enabling adaptive behavior such as
119 metabolic switching or change in kinetics due to mutations. (4) Agent properties can now be assembled
120 from orthogonal modules giving the user pick and mix flexibility. The same is true for processes. Thus,
121 the complexity of agents or processes can be adjusted to fit the modeling purpose. Due to the modular
122 structure, it has become easier to implement novel functionality. (5) Force-based mechanical
123 interaction framework enabling attractive forces and non-spherical agent morphologies, which was
124 impossible with the shoving algorithm. We showcase this new feature in a case study demonstrating
125 how the fitness of filaments benefits from escaping competition.

126 Model development and description

127 The description of iDynoMiCS 2.0 and the case studies presented in this paper follow the ODD
128 (Overview, Design concepts, Details) protocol for describing individual- and agent-based models
129 [24,25]. However, iDynoMiCS 2.0 is not one specific model but a platform to facilitate the specification
130 of a broad variety of models. Hence, this section aims to provide a general description of the platform
131 but cannot cover all possible models that could be simulated. Thus, we also provide detailed model-
132 specific ODD descriptions together with the presented case studies.

133 Overview

134 The purpose of iDynoMiCS 2.0 is to facilitate the simulation of large groups of individual microbes and
135 their interactions in a microbial population or community, either in a well-mixed chemostat-like or a
136 spatially structured biofilm-like compartment. The aim is to study and predict how the interactions and
137 properties of individual microbes lead to emergent properties and behaviors of microbial
138 communities.

139 Entities, state variables and scales

140 Entities, state variables and scales may vary from one model implementation to another. In a typical
141 implementation, microbial cells are the principal agents. They can mediate both chemical and physical
142 activities. Agents can have any number of properties and behaviors. Typical properties are position,
143 mass, density, shape, composition and metabolic reactions. Typical behaviors are cell growth, division,
144 death, extracellular polymeric substance (EPS) production and excretion. iDynoMiCS 2.0 refers to
145 properties and behaviors of an agent as the “aspects” of an agent. Shared aspects can be set-up as a
146 module and reused for all agents sharing these aspects. A typical agent is one or multiple orders of
147 magnitudes smaller than the computational domain.

148 The simulated space (computational domain) in which agents reside is called a compartment. There
149 are two types: spatially explicit compartments in 2D or 3D to simulate microbial assemblages such as
150 biofilms and well-mixed compartments used to simulate the dynamics of a bulk liquid without agents
151 or a planktonic community with or without inflows and outflows (batch, fed-batch or chemostat);
152 these compartments are assumed to have no spatial structure and thus the concentrations of chemical
153 species and agents are homogeneous.

154 Well-mixed and spatially explicit compartments may be connected to simulate how bulk and biofilm
155 dynamics are coupled. Compartments can have multiple properties including: boundaries, physical
156 dimensions, volume and a scaling factor. This scaling factor is used to translate between the size of a
157 simulated representative volume element and the actual size of the system, it allows a smaller
158 simulated compartment to represent a larger entity. There are no hard restrictions on compartment
159 size, however, compartments typically have lengths up to a millimeter. Agents can only reside in a
160 single compartment at any one time, but they can be transferred or move between spatially explicit
161 and well-mixed compartments.

162 Dissolved chemical species in iDynoMiCS 2.0 are referred to as solutes. Compartments can contain any
163 number of solutes. In well-mixed compartments, a solute is represented as a single concentration. In
164 spatially explicit compartments, solutes are represented as 2D or 3D concentration fields in a Cartesian
165 grid. The distance between grid nodes is referred to as the resolution, typically one to a few
166 micrometers.

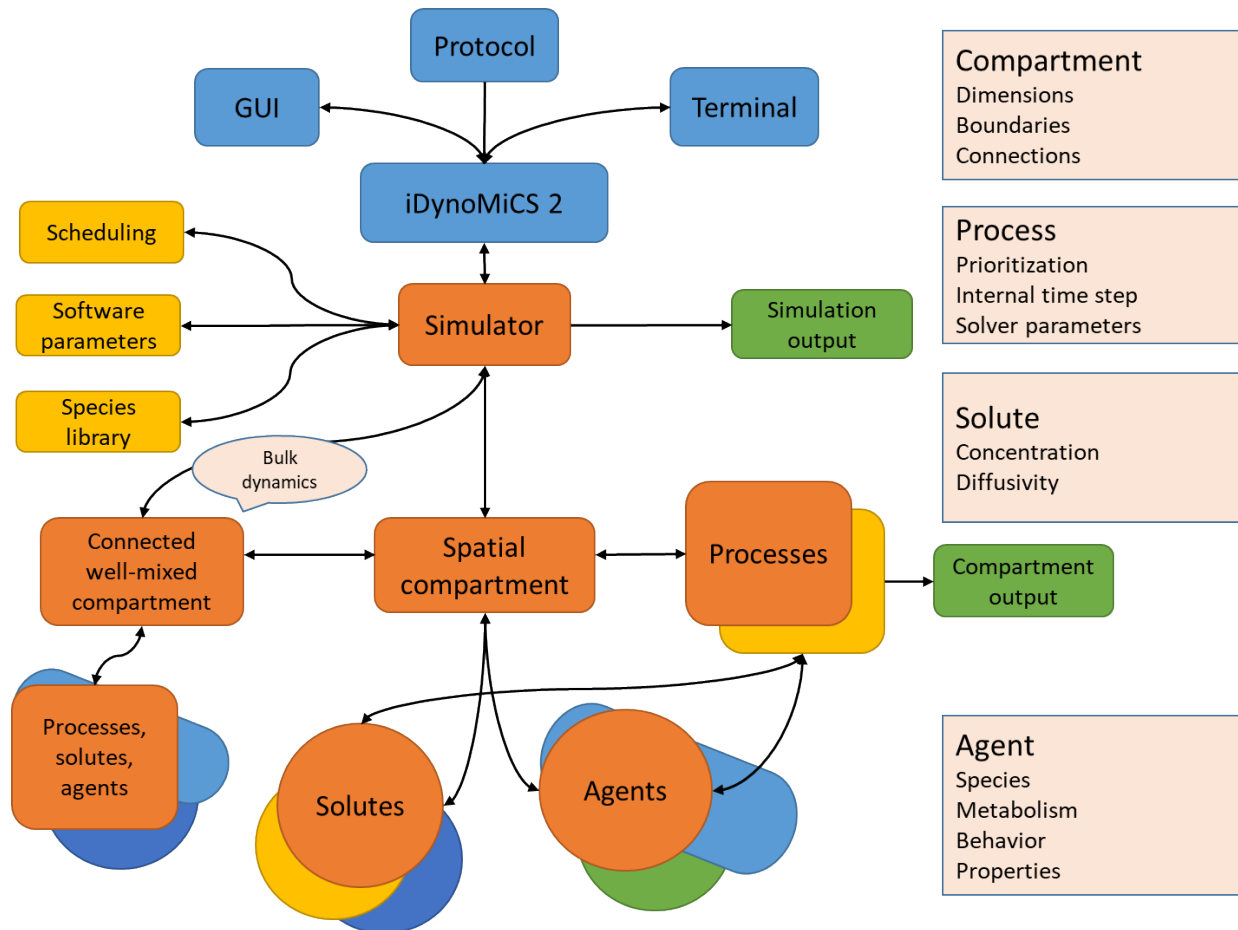
167 Framework structure

168 In iDynoMiCS 2.0, models are structured, specified and instantiated hierarchically. The basic structure
169 of a typical scenario is presented in Fig 1. The “Simulator” is the root of any model implementation. It
170 loads the model specification from a protocol file provided by the user either through the GUI or the
171 command terminal. General software control parameters are managed at the simulator level, as well
172 as the scheduling of sub-models, the management of compartments and the storage of species
173 modules (reusable sets of aspects). The simulator steps through its compartments and saves the model
174 state at each global time-step. A compartment stores its shape and size, solutes and agents in the
175 compartment and processes occurring within the compartment. Agents and processes store their
176 properties as aspects. This layered structure of model input provides a level of modularity to the
177 iDynoMiCS 2.0 software and model implementations.

178 Modularity enables flexible combination and facilitates software maintenance and development. An
179 iDynoMiCS 2.0 model is formulated as distinct modules describing specific parts of the model such as
180 a compartment, process or an agent. An example model description is included in Box 2. These
181 modules can be referenced to add the same object, property or process in another compartment or
182 agent. For example, multiple agents of different species can implement the same module describing
183 cell shape but implement a different module describing metabolism.

184 Within the software, modularity is implemented through the use of software interfaces and
185 abstractions. These software interfaces ensure common functionality such that loading or storing of
186 data, scheduling and initiation are handled in the same way for any software class implementing these
187 interfaces. This concept makes it easier to add new features and extensions to iDynoMiCS 2.0, since
188 an extension can be integrated into the framework without additional work to handle initiation, data
189 handling, scheduling and other auxiliary functionality (Box S1).

190 Support for arithmetic and basic logic expressions provides flexibility to iDynoMiCS 2.0 models. Users
191 can simulate any type of kinetic or physical interaction model that can be described by a standard
192 arithmetic expression. Logic expressions are particularly useful in models with biological switches or
193 thresholds. Typical examples are metabolic or morphological switches. Since any kind and number of
194 aspects can be changed, the characteristics of an agent can completely change at runtime. Logic
195 expressions can also be used to filter agents matching specific criteria, which can be useful for further
196 analysis, or to color agents based on their properties. Logic expressions may incorporate arithmetic
197 expressions.



198
199

200 **Fig 1. The basic structure of an iDynoMiCS 2.0 model.** Interaction with the program takes place
 201 through the GUI or command line terminal. A protocol file specifying a model can be loaded to initialize
 202 the simulator. If parameters are missing from the protocol file, a default is loaded or the user is queried
 203 if no default exists. Scheduling ensures predictable handling of the compartments and the order of
 204 processes occurring within them. A species library is kept such that properties and/or behavior that
 205 are identical for agents of the same species can be looked up from the library. The simulator further
 206 ensures that the model state is saved at the end of each global time step. Spatially explicit and well-
 207 mixed compartments can be connected. Solutes concentration fields are stored as matrices, which
 208 include local solute concentrations, local diffusivity and reaction rates. The collective of agents
 209 represents the biofilm, agents may have many properties depending on user specifications, basic
 210 properties are species, mass and position of the agent. Processes act upon the information in the
 211 model system and describe the processes occurring in the model such as mechanical interactions or
 212 diffusion, or generate output from the active model state.

213 [Process overview and scheduling](#)

214 Many processes can take place in a microbial community, often simultaneously. To capture these
 215 processes in a computer model, they are represented by simplified mathematical models, discretized
 216 and handled in an asynchronous fashion. An iDynoMiCS 2.0 simulation steps through a number of
 217 global time-steps. Within each global time-step and for each compartment, sub-models describing
 218 activities occurring in the microbial community are executed. Processes included in a model depend
 219 on the purpose and design of the model. However, most simulations include: physical interactions,
 220 (bio-)chemical reactions, diffusion of chemical species, microbial growth and cell division. A detailed
 221 overview of implemented submodels follows later.

222 During one global time step, a list of processes, defined and scheduled by the user, are executed. Each
223 process is assigned a time step size and a priority by the user, if not, the global time step and order of
224 occurrence in the protocol file are adopted as time step and priority. A process can be repeated during
225 a single global time step and may have smaller internal time steps. Processes are handled in a specific
226 order; the process time step is used to determine what process is due first. If multiple processes are
227 due simultaneously, the process priority is used to determine the order. Box 1 shows a scheduling
228 example as implemented in the biofilms promote altruism case study presented later.

229 **Box 1. Process schedule for the biofilms promote altruism case study within a single global time**
230 **step.**

- 1) (Bio-)chemical reactions and diffusion
 - a. Update solute grids and agent masses (e.g. (bio-)chemical conversion)
 - b. Update solute boundaries
- 2) Agent updates
 - a. Cell division
 - b. Differentiate (switch between sphere or rod shaped if applicable)
 - c. Update cell size
- 3) Mechanical relaxation
 - a. Update cell positions and mechanical stresses until relaxation criteria are met
- 4) Compartment reporting
 - a. Density grid (csv)
 - b. Compartment summary (csv)
 - c. Graphical output (pov/svg)
- 5) Save simulation state (xml/exi)

231

232 **Design concepts**

233 *Basic principles:* Microbes are modeled as individual particles that interact with their environment.
234 Mass is conserved and thus the mass balance of any 'element' in the model system should be closed.

235
$$in + production - out - consumption = 0 \quad (1)$$

236 *Emergence:* System-level phenomena such as the distribution of microbial agents, the spatial structure
237 of a biofilm, and chemical conditions all emerge from interactions between agents and their local
238 environment. This local environment can consist of other agents, local chemical concentrations or a
239 local surface.

240 *Adaptation:* iDynoMiCS 2.0 models can include adaptation. By sensing the local environment or
241 internal states, an agent may change its characteristic using the differentiate aspect. Adaptation can
242 also be stochastic, where heritable stochastic changes in an agent's characteristics can lead to selection
243 of the lineage best suited to survive or thrive in the simulated environment.

244 *Objectives:* Agents can have objectives. For example, agents may have the objective to move to a
245 region with higher substrate availability (chemotaxis).

246 *Learning and prediction:* Although microbes have no brain, they can have memory and process signals.
247 For example, chemotaxis requires memory. Also, event occurrences may be stored as an aspect of the
248 agent and influence the behavior or characteristics of an agent.

249 *Sensing*: Locally sensed nutrient concentrations can affect growth rate or adaptation. Neighboring cells
250 may affect the spatial direction of cell division in filamentous agents or affect physical displacement. A
251 combination of the above supports microbial behaviors such as dormancy or chemotaxis.

252 *Interaction*: Agents interact with their local environment by consuming and producing solutes,
253 including extracellular enzymes, or particles such as EPS. As a consequence, they indirectly interact
254 with neighboring agents, leading to competition, cooperation or communication. The agents further
255 interact with their physical environment by pushing or pulling other physical entities, including other
256 agents as well as physical surfaces in the computational domain.

257 *Stochasticity*: Model implementations can include stochastic processes, examples are allocation of
258 biomass to daughter cells upon cell division, placement of daughter cells relative to the position of the
259 mother cell, stochastic movement (for example Levi flight), and mutations or other random
260 perturbations. A random seed is saved so simulations can be continued with consecutive random
261 numbers or repeated with an identical series of random numbers if desired.

262 *Collectives*: Microbes may aggregate actively through motility coupled with communication and the
263 expression of surface proteins or passively through cell division and the production of an extracellular
264 matrix [26]. Consequently, agents can form a local collective of unrelated or related cells. Moreover,
265 communication can coordinate collective action that does not require aggregation. iDynoMiCS 2.0 has
266 the basic building blocks to model coordinated collective behavior such as quorum sensing.

267 *Observation*: The model state is saved at the end of each global time-step. Additional compartment
268 output can be saved, including physical and biological states of all agents and the chemical state, at
269 any given time and location in the simulation.

270 Initialization

271 The initial state of a simulation is highly flexible and should be provided by the user. This includes
272 solute concentrations as well as positions and states of agents, which may be based on experimental
273 data or generated to investigate hypothetical scenarios. iDynoMiCS 2.0 includes several helper classes
274 to generate initial states. A ‘random spawner’ can be used to randomly distribute large numbers of
275 agents of a certain type over a pre-defined region, applied in the initialization of the stress test and
276 Benchmark 3 case study. A ‘distributed spawner’ has a similar function but distributes agents regularly
277 at a pre-defined interval, applied in the initialization of the biofilms promote altruism case study. It is
278 also possible to manually define an initial state for any individual or to utilize a previous simulation
279 outcome as an initial state for a new simulation, for example to implement a perturbation.

280 Input

281 All simulations are initiated using iDynoMiCS 2.0 protocol files. They follow the logical structure of the
282 model setup and are structured using the Extensible Markup Language (XML). Both XML and EXI
283 (Efficient XML Interchange) files can be used. It is recommended to include units when specifying
284 parameters in the protocol file, units are converted to iDynoMiCS’s base unit system, which avoids unit
285 conversion mistakes.

286 **Box 2. An abbreviated protocol file showing the hierarchical structure.** Setting up a basic protocol is
287 relatively simple and supported by the GUI. In this example, 30 copies of an agent of species
288 “bacterium” are added to a rectangular domain. Bacterium is defined by the reusable “coccooid” aspect
289 highlighted in green as well as a growth reaction which is only used for this species. The coccooid module
290 describes basic physical properties and behavior of a generalized coccooid including agent density,
291 division mass, etc. Bacterium contains the “reactions” aspect which is a list of all reactions the agent
292 can catalyze (in this case only the crucial growth reaction). The reaction node includes an arithmetic
293 expression defining the growth kinetics based on the local solute concentrations of two solutes (carbon
294 and oxygen) and associated kinetic constants and stoichiometry. The protocol further describes the
295 properties of the compartment, the solutes and processes to be loaded. The full protocol file is just 60
296 lines and included in S1.7.

```
<simulation name="simple_biofilm" outputfolder="../results" log="NORMAL">
  <timer stepSize="3 [h]" endOfSimulation="10 [d]" />
  <speciesLib>
    <species name="bacterium">
      <speciesModule name="coccooid" />
      <aspect name="reactions" class="InstantiableList">
        <list nodeLabel="reaction" entryClass="RegularReaction">
          <reaction name="growth">
            <expression value="mass * mumax * (carbon / (carbon+Ks)) * ((oxygen / (oxygen+Kox)))">
              <constant name="Ks" value="2.4 [g/m+3]" /> // additional constants
              <stoichiometric component="oxygen" coefficient="-18.0" /> // additional stoichiometry
            </expression>
          </reaction>
        </list>
      </aspect>
      <species name="coccooid">
        <aspect name="density" class="Double" value="0.15" />
        <aspect name="divisionMass" class="Double" value="0.2 [pg]" />
        <aspect name="morphology" class="String" value="coccooid" /> // additional aspects
      </species>
    </speciesLib>
    <compartment name="biofilm-compartment">
      <shape class="Rectangle">
        <dimension name="X" isCyclic="true" targetResolution="2.0" max="32.0"/>
        <dimension name="Y" isCyclic="false" targetResolution="2.0" max="64.0">
          <boundary extreme="1" class="FixedBoundary" layerThickness="32.0">
            <solute name="oxygen" concentration="8.74 [mg/l]" /> // additional fixed boundary solutes
          </boundary>
        </dimension>
      </shape>
      <solutes>
        <solute name="oxygen" concentration="8.74 [mg/l]" defaultDiffusivity="2000.0 [um+2/s]"/> //
      </solutes>
      <agents>
        <spawn class="randomSpawner" domain="32.0, 1.0" number="30" morphology="COCCOID">
          <templateAgent>
            <aspect name="species" class="String" value="bacterium" />
            <aspect name="mass" class="Double" value="0.2 [pg]" />
          </templateAgent>
        </spawn>
      </agents>
      <processManagers>
        <process name="agentRelax" class="AgentRelaxation" priority="0" />
        <process name="PDEWrapper" class="PDEWrapper" priority="1" />
      </processManagers>
    </compartment>
  </simulation>
```

297

298 Output

299 The model state is saved as XML or EXI file to reduce file size after each global time step and follows
300 the same structure as a protocol file. The output also includes all information required to restart the
301 simulation. It is also possible to save additional output per compartment to facilitate later analysis or
302 visualization. Visual output includes SVG or POV formats to render the agents in a compartment. The
303 hue, saturation or brightness of the agent can be adjusted based on its properties to convey additional
304 information about the agent’s state. A CSV file listing agents with key properties of interest can also
305 be produced, this list can be filtered to only include agents matching specific criteria. Further, the
306 density of agents in the compartment can be reported for all agents or those matching specific filters
307 (such as belonging to a certain species). Finally, a summary with key statistics on the compartment can
308 be written such as mean solute concentrations, total agent counts and masses, agents matching
309 specific criteria, etc. The summary is useful to quickly plot time series data.

310 User interface

311 Simulations can be loaded and started through the command line or a GUI (Fig S9), which may be used
312 to review, edit or create protocol files before running them. During the simulation, the GUI provides
313 key information on the simulation state (such as substrate concentrations, species abundance,
314 convergence of the reaction diffusion solver, etc.). The spatial domain can be rendered directly to
315 display agent distributions and concentration gradients. Lastly, the GUI can be used to extract key data
316 from iDynoMiCS 2.0 output files, convert between EXI and XML files and convert numbers between
317 different unit systems including SI and iDynoMiCS 2.0 base units.

318 Submodels

319 Here we describe key submodels currently implemented in the iDynoMiCS 2.0 platform. Specific model
320 implementations may utilize a subset of these submodels or alternative submodels that extend
321 capabilities further.

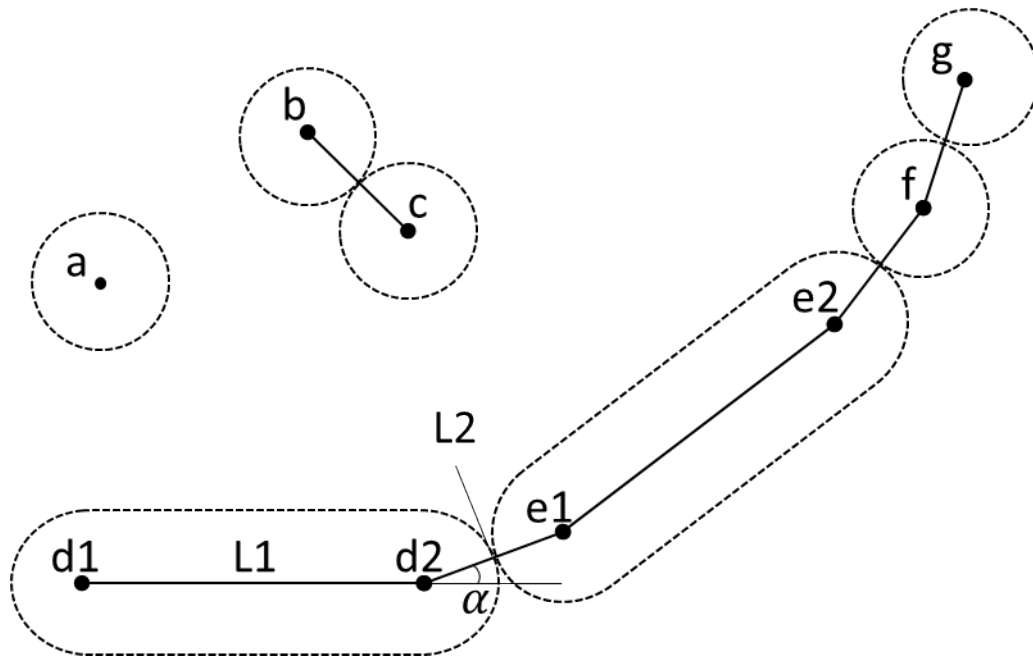
322 *Physical representation of agents*

323 Microbial cells in the model have position and extent in 3D continuous space, constructed from points
324 and swept-sphere volumes (Fig 2). Specifically, spherical cells dubbed “cocci” are constructed from a
325 single point with a spherical volume, rod-shaped cells dubbed “bacilli” are constructed from two points
326 connected by a line-segment and a swept-sphere volume along the line-segment, filaments are
327 represented as a chain of either one or both. Every point has a mass associated with it.

328 In order to simulate 2D models, a number of assumptions and adjustments have to be made. An
329 implicit third dimension (z) is required to retain consistency for physical units such as volume or
330 concentration, in iDynoMiCS 2.0 this third dimension is 1 μm thin. The 2D agent shapes are extruded
331 into this virtual dimension, thus their pseudo 3D shapes have a uniform cross-sectional area and a
332 thickness of 1 μm . This translation from 3D to 2D comes with several side effects such as a lower
333 density of circle packing as compared to sphere packing [27]. To mitigate this effect, Clegg et al. [27]
334 proposed a density scaling factor of 0.82 for 2D simulations with spherical agents. Appropriate scaling
335 factors for other agent shapes or mixtures of agent shapes are unknown.

336 Another side effect of 2D simulations results from the constraint that the length of the virtual third
337 dimension has to be identical for all agents. This can result in unwanted agent size effects for agents
338 with very small or large radii. iDynoMiCS 2.0 can scale the density of agents in order to retain consistent
339 agent diameters and lengths between 3D and 2D simulations. This method is described in detail in
340 S1.12. This method is not a perfect solution as it will introduce new side effects, the local shifts in
341 biomass concentrations will increase nutrient competition for large agents whilst decreasing for small
342 agents. If there are large differences in agent size, it is recommended to test validity of 2D simulations
343 with 3D simulations.

344 Additionally, biofilm structure and development can be affected in 2D simulations. Vertically stratified
345 biofilms with chemical gradients from substratum surface to the biofilm-liquid interface dominating,
346 or biofilms with gradients in the second dimension, parallel to the substratum surface, that are
347 equivalent in the third dimension which is also parallel, can be accurately modeled in 2D. However,
348 biofilms that form finger-like or other superstructures become artificially substrate limited due to the
349 lack of mass transport in the third dimension. Consequently, these superstructures will form under
350 different environmental conditions in 2D versus 3D.



351

352 **Fig 2. Different agent shapes in iDynoMiCS 2.0.** Dashed lines indicate sphere-swept volumes of 'dots'
353 or line-segments. Dots are mass-points indicating position and orientation of agents. Solid lines
354 indicate mechanical interactions between points (forces between points modeled as springs): Collision
355 interaction (b-c), spine interaction responsible for the rigidity of rod-shaped agents (d1-2 and e1-2),
356 connecting interactions (d2-e1, e2-f, f-g). α is the angle between two elements of a filament. This angle
357 can be counteracted by a torsion spring applying forces on d1, d2 and e1. L1 and L2 are the moment
358 arms. The torsion spring applies force until the angle α reaches 180° , aligning the three points.

359 *Mechanical interaction framework*

360 In the original iDynoMiCS 1, agent overlap was resolved with a shoving algorithm. In iDynoMiCS 2.0,
361 mechanical interactions between agents (or with surfaces in their environment) as well as between
362 different points within the same agent is based on forces. This Force-based Mechanics (FbM)
363 framework builds on the mass-spring models of Janulevicius *et al.* [28], Celler *et al.* [29] and Storck *et al.* [30]
364 but is no longer limited to spring forces. The shoving algorithm is still available as an alternative
365 or for comparison with iDynoMiCS 1.

366 Before an interaction force can be calculated, the interaction needs to be detected. Direct links
367 between two points of the same agent are stored as an aspect of the agent. Additionally, neighboring
368 entities are found efficiently through a search of the quad- or octree that keeps agents spatially sorted.
369 Through collision detection, as described and implemented by [31] and [30], physical interaction
370 between neighboring agents is tested. The distance between two objects (which can be negative) is
371 used in a force model to calculate the resulting force of the interaction. The quad-, octree and collision
372 detection algorithms were modified to work with periodic boundaries.

373 *Forces*

374 The FbM solver exploits the fact that under conditions of very low Reynolds numbers, inertial forces
375 on a particle become negligible [32,33]. Because of this, the sum of all forces applied to the mass-point
376 (the net force $\sum F_p$) can be assumed to balance the mass-point's drag force F_D ($F_D = \sum F_p$) near
377 instantly. By applying Stokes' law, the terminal velocity of the mass-point v_t can be obtained, under
378 low Reynolds number conditions the mass-point reaches this velocity near instantly and thus we can
379 assume $v \approx v_t$ when $Re \ll 1$ (Eq 2) [34]. This simplification effectively halves the number of ordinary
380 differential equations that need to be solved.

$$381 \quad v \approx v_t = \frac{\sum F_p}{6\pi r_c \mu_f} \quad (2)$$

382 With r_c the diameter of the cell and μ_f are the dynamic viscosity of the fluid.

383 The mass-point's velocity, and by extension the point displacement, is resolved using a forward Euler
384 method or the second-order Heun's method [35].

385 Multiple types of interactions may lead to a net force being exerted on any given point. These forces
386 may be due to collision, close proximity repulsion or attraction, attachment and internal structure. A
387 force model for these interactions can be provided through the protocol file. Default models are used
388 if no model is provided. The default force model for agent collision is the Hertz soft sphere model [36]
389 (Eq 3), where r_{eff} is the effective radius, E_{eff} the effective Young's modulus and ξ the agent overlap.

$$390 \quad F = \frac{4}{3} \sqrt{r_{eff}} E_{eff} \xi^{3/2} \quad (3)$$

391 Rod-shaped cells and filaments have permanent connections between points (L1 & L2 in Fig 2). By
392 default, these connections are modeled as linear springs following Hooke's law (Eq 4), where k is the
393 spring constant and δl the difference between the current length and the rest length.

$$394 \quad F = k\delta l \quad (4)$$

395 An internal force can also be specified to resist bending, for example for segments of a filament (Angle
396 α in Fig 2). The default model for such torsion springs is the angular form of Hooke's law (Eq 5), where
397 κ is the spring constant, $\delta\theta$ the difference between the actual angle and rest angle, L the length of the
398 momentum arm.

$$399 \quad F = \frac{\kappa\delta\theta^2}{L} \quad (5)$$

400 Forces for agents in proximity can also be specified, for example, close range repulsion and/or
401 attraction, but are not applied by default.

402 *Reactions*

403 A reaction transforms chemicals; these chemical species may be modeled explicitly as solutes or types
404 of the structured biomass within cells (e.g., regular biomass and storage compounds), or implicitly and
405 so left out of the model description (e.g., water in aqueous environments). Reactions have a rate and
406 stoichiometry. They may be catalyzed by agents or occur independently of agents in the environment.

407 Reaction rates may depend on the concentration of certain reactants, such as solutes or biomass, and
408 other variables, such as temperature. Within iDynoMiCS 2.0, rate equations can be expressed through
409 any type of arithmetic expression, which allows the use of almost any kinetic model, not only Monod
410 type kinetics but also thermodynamics-based kinetics such as the models by Rittmann and McCarty

411 [37] or Heijnen [38]. Such a thermodynamics-based lbM approach was previously implemented by
412 Gogulancea et al. [39]

413 Positive stoichiometry signifies production, and negative stoichiometry consumption, when the
414 reaction proceeds in the forward direction (has a positive rate). Thus, the production rate of a solute,
415 i , by reaction, j , is given by:

$$416 \quad q_{i,j} = N_{i,j} r_j \quad (6)$$

417 where N denotes stoichiometry and r denotes reaction rate.

418 *Solutes in well-mixed environments*

419 In compartments assumed to be well-mixed, there is no spatial structure for solutes nor for agents.,
420 thus the rate of change is an ordinary differential equation summing inputs, outputs and reactions

$$421 \quad \frac{d}{dt} S_s(t) = \sum_{i \in \text{inflows}} D_i S_{s,i}(t) - \sum_{i \in \text{outflows}} D_i S_s(t) + q_s(t) \quad (7)$$

422 where $S_s(t)$ is the concentration of solute s at time t and D_i the dilution rate for a given inflow/outflow.
423 The production rate expression $q_s(t)$ combines environmental reactions, $q_{s,env}$, with reactions catalyzed
424 by each agent, $q_{s,agent}$.

$$425 \quad q_s(t) = q_{s,env}(S(t)) + q(S(t),agents(t)) \quad (8)$$

426 where $S(t)$ is the local solute concentration.

427 *Diffusion-Reaction of solutes*

428 Within spatially explicit compartments, the dynamics of solutes are governed by two processes: Fickian
429 diffusion and reactions.

430 For each solute, the rate of change for each solute is now given by the elliptic Partial Differential
431 Equation (PDE) that combines Fickian diffusion, given by the divergence div of the diffusional flux
432 driven by the concentration gradient ∇S_s , and reaction [40].

$$433 \quad \frac{\partial}{\partial t} S_s(\mathbf{x},t) = \text{div}(\omega_s(\mathbf{x}) \cdot \nabla S_s(\mathbf{x},t)) + q_s(\mathbf{x},t) \quad (9)$$

434 where \mathbf{x} is the spatial position, ω_s is the local diffusivity, and $S_s(\mathbf{x},t)$ the local concentration of solute s .
435 Dynamics at compartment edges are governed by boundary conditions.

436 As in iDynoMiCS 1 [17] and other biofilm models, a pseudo steady-state assumption is made to model
437 solute dynamics because reaction and diffusion processes are several orders of magnitude faster than
438 biomass growth, decay and detachment processes [41]. Hence, reaction and diffusion rates rapidly
439 reach a pseudo steady-state while the biomass distribution is changing so slowly that it can be
440 considered 'frozen' [42]. This time scale separation drastically reduces the computational demand of
441 the simulation but it should be checked whether the pseudo steady-state assumption is reasonable.

442 *Boundaries*

443 Spatially explicit compartment boundaries can be of different types. (a) Solid boundaries where neither
444 agents nor solutes can pass through (Neumann or no flux boundary condition). (b) Fixed concentration
445 or Dirichlet boundary conditions where the solute concentrations are fixed to preset values or
446 determined dynamically by an ODE such as Eq 7 for a connected well-mixed compartment. (c) Periodic
447 boundaries where agent and solutes can move through the boundary to the opposite side of the
448 domain, which ensures identical concentrations on each side to avoid edge effects.

449 Well-mixed compartments may also exchange solutes and agents with other well-mixed or spatially
450 explicit compartments through its boundaries. (d) A boundary connecting a spatially explicit with a
451 well-mixed compartment, where solute concentration gradients in the spatially explicit compartment
452 result in a diffusive flux through the boundary determined by the concentration gradient at the
453 boundary. (e) An inflow boundary with preset solute concentrations and flow rate. (f) An outflow
454 boundary with the concentrations matching the content of the well-mixed compartment and a preset
455 flow rate, which may match the inflow. The well-mixed compartment may change volume over time if
456 inflow and outflow rates do not match. An outflow boundary can be set to retain the agents present
457 in the well-mixed compartment to model biomass retention in a retentostat.

458 *Plasmid Dynamics*

459 Plasmid dynamics incorporates conjugative transfer and segregative loss of plasmids. Plasmids are
460 included as aspects of an agent, with loss defined as an event occurring upon agent division. The
461 dynamics of conjugation modeled here follow the known behavior of F-pili driven plasmid transfer
462 described in S1.11.

463 Results

464 We start by summarizing the strategy and results of our model verification efforts that were focused
465 on comparing our numerical solvers against analytical solutions in the simpler test cases and well
466 tested solvers implemented in other software in the more complex test cases. This is followed by using
467 benchmarks. First the standard Benchmark 3 for comparison of biofilm models as previously done for
468 iDynoMiCS 1. Then a second, new benchmark that is highly sensitive to initial conditions and spatial
469 structures due to positive feedbacks where we can compare iDynoMiCS 2.0 results with BacSim and
470 also investigate the often-neglected effect of different biofilm spreading mechanisms. Finally, we
471 demonstrate some of the new capabilities of iDynoMiCS 2.0 – simulating filaments which requires FbM
472 – and show some surprising new results.

473 Model verification and performance

474 Component testing and solver verification

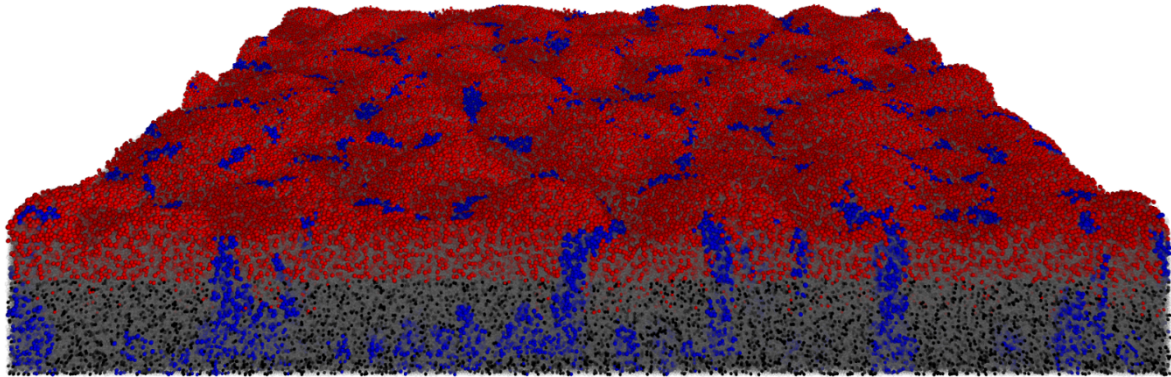
475 iDynoMiCS 2.0 has undergone a rigorous verification process. We focused on numerical solvers, writing
476 code to inspect the state at each iteration and diagnose convergence of solvers. This process helped
477 eliminate bugs and software inefficiencies. It also demonstrated solutions were numerically correct
478 with deviations of <0.1% in all test scenarios with known analytical solutions. The testing process
479 included single-component testing (or unit testing), multi-component testing, stress testing and
480 benchmarking, following a strategy of increasingly complex test scenarios where analytical solutions
481 were known for simpler cases, numerical solutions from well-tested other solvers for intermediate
482 cases and comparison to output of a set of other models for the most complex test cases. Single-
483 component testing entailed the testing of individual parts of the framework against known solutions
484 or predicted convergence. This included tests for collision detection and collision response (S1.2),
485 (bio-)chemical conversion and material transport in a well-mixed compartment (S1.3), microbial
486 growth in a well-mixed compartment (S1.3) and (bio-)chemical conversion and diffusion in a spatially
487 explicit compartment (S1.3).

488 Multi-component testing where multiple parts of the framework are tested simultaneously was
489 performed through using various test scenarios. The goal of these tests was to see whether multiple
490 components worked correctly in unison and whether iDynoMiCS 2.0 can perform more complex
491 scenarios stably and reproducibly. Test scenarios are listed in S1.9, protocol files for all scenarios are
492 available on the iDynoMiCS 2.0 GitHub repository.

493 **Stress testing**

494 Stress testing built on multi-component testing, but tested scalability of performance and pushed the
495 limits of domain size. In the process, software limitations and bottlenecks were removed. The stress
496 test verified that iDynaMiCS 2.0 was capable of simulating the development of a 3D biofilm over 175
497 simulated days to reach >10 million agents (Fig 3, detailed description in S1.4) in 11.34 days on a single
498 processor.

499

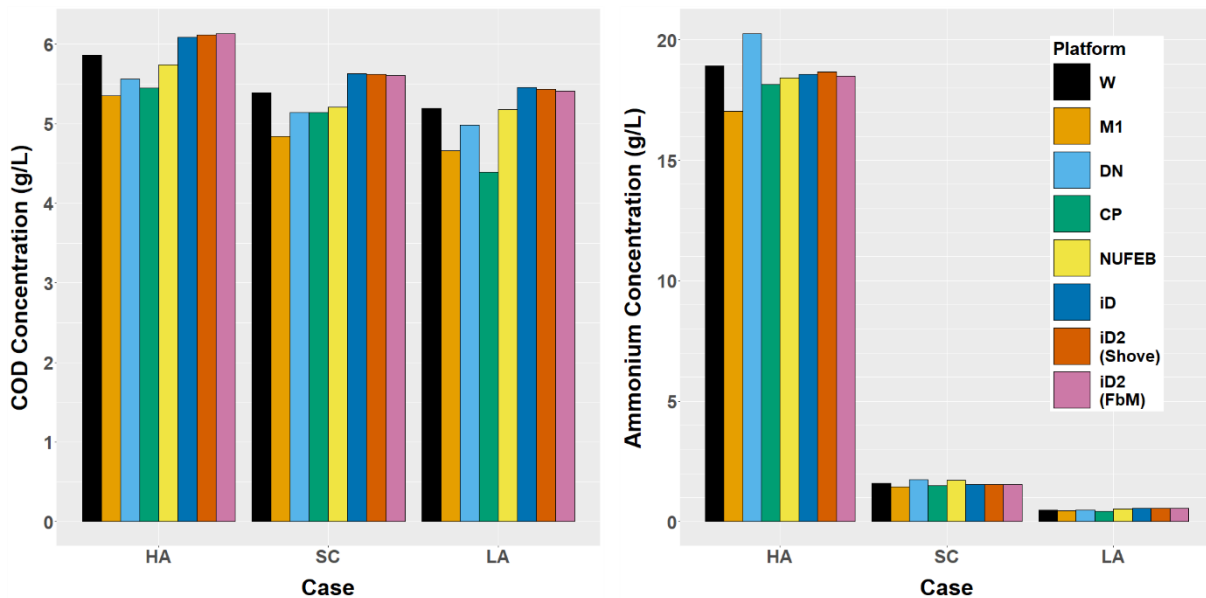


500

501 **Fig 3. iDynaMiCS 2.0 was capable of simulating large 3D biofilms.** A nitrifying biofilm was initiated
502 with 1,000 Ammonium Oxidizing Organisms (red) and 1,000 Nitrite Oxidizing Organisms (blue) in a
503 500x500x500 μm domain. Both species produced EPS particles (gray semi-transparent). Agents that
504 dropped below 20% of their division mass as a result of endogenous respiration (maintenance
505 metabolism) became inactive (black). The 175-day biofilm contained 1.02×10^7 agents (bacteria and
506 EPS particles).

507 Benchmarking against various types of biofilm models

508 iDynoMiCS 2.0 was benchmarked against 1D or 2D continuum models, 2D Cellular Automata and 2D
509 particle-based models including iDynoMiCS 1, using the multi-species nitrifying biofilm Benchmark
510 Problem 3 or BM3 [43,44]. BM3 was the most complex benchmark developed by the International
511 Water Association biofilm modeling task group to compare computational modeling approaches for
512 biofilms and provide guidance for researchers. All models implemented the same processes.
513 Unfortunately, some published BM3 results are limited to steady state concentrations of organic
514 carbon (expressed as Chemical Oxygen Demand, COD) and ammonium in the bulk liquid that
515 exchanges with the biofilm so we could only show that these results from iDynoMiCS 2.0 did not differ
516 significantly from the distribution of results from the other models (Fig 4, Table SI9). iDynoMiCS 1 was
517 previously shown to produce similar results to another particle-based model, NUFEB [21,45]. We also
518 tested and confirmed that the physically realistic biomass spreading mechanism FbM in iDynoMiCS 2.0
519 gave similar results to the biomass spreading by shoving in iDynoMiCS 1, and for that purpose
520 implemented shoving in iDynoMiCS 2.0 as well (Fig 4). Since FbM produces denser biofilms (in the
521 absence of EPS particles that would distance cells explicitly), biofilm density had to be scaled
522 accordingly for this comparison. An extensive BM3 description and results analysis is included in S1.5.



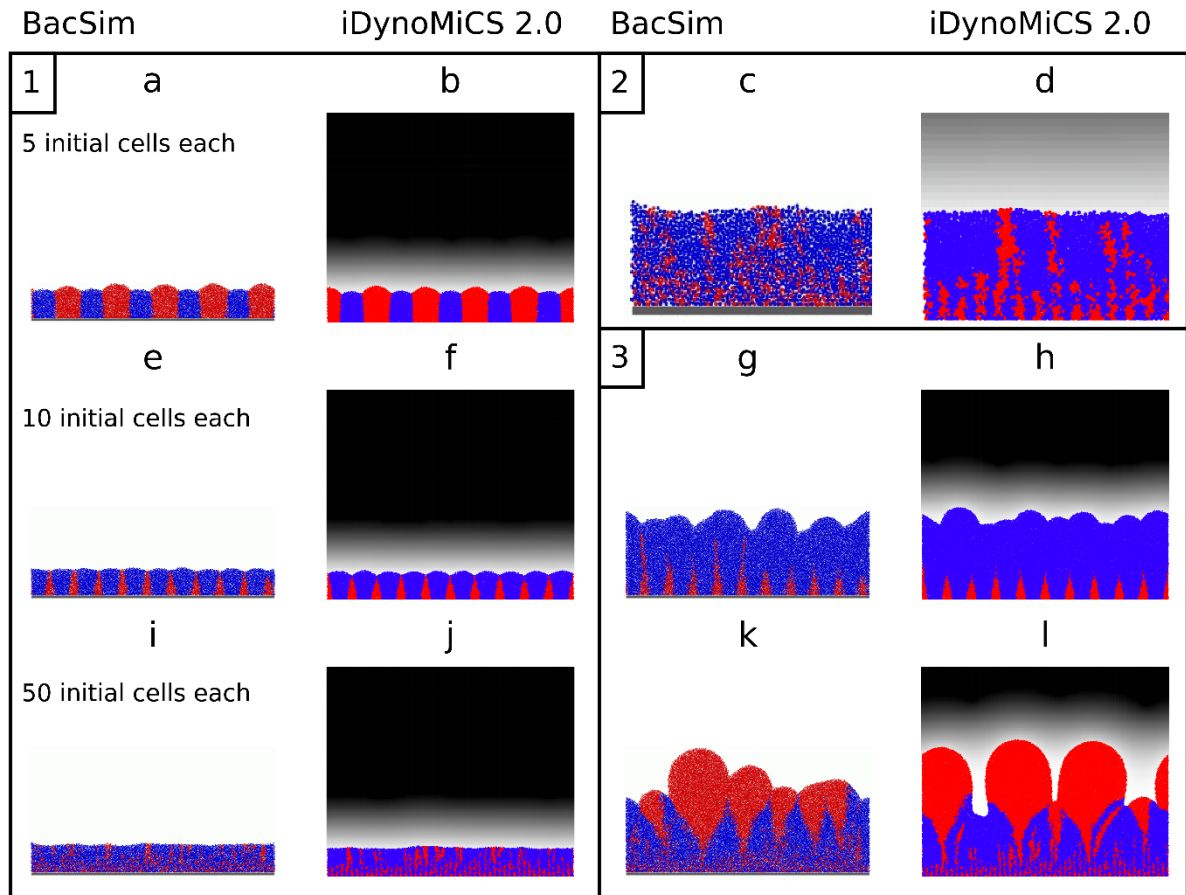
523

524 **Fig 4. Comparing steady states in BM3.** Steady state organic carbon (Chemical Oxygen Demand,
525 COD) and ammonium concentrations in the bulk liquid for the three different BM3 cases (HA: High
526 ammonium, SC: Standard case, LA: Low ammonium) across 7 model implementations (W: Wanner,
527 M1: Morgenroth, DN: Dan Noguera, CP: Cristian Picioreanu, NUFEB: NUFEB, iD: iDynoMiCS 1, iD2:
528 iDynoMiCS 2.0, either with shoving algorithm similar to iD or the new Force-based Mechanics).

529 Comparing the effect of different biomass spreading mechanisms: Biofilms promote
530 altruism case study

531 As a second and new benchmark for model testing and comparison, we have chosen a biofilm scenario
532 where a positive feedback can amplify initially small differences leading to divergent results. This was
533 thus a good opportunity to examine the effect of different biomass spreading mechanisms, comparing
534 BacSim, the first implementation of shoving for biofilms [46] with iDynoMiCS 2.0. The scenario
535 consisted of competing two growth strategies, a Rate Strategist (RS) that grew faster at every substrate
536 concentration (higher μ_{max} , same specific affinity/initial slope of the Monod kinetics) but had a lower
537 growth yield, with a Yield Strategist (YS) that grew more slowly but had a higher growth yield and
538 therefore converted the substrate diffusing into the biofilm with higher efficiency into biomass. This
539 more economical use of resources is an example of altruistic behavior as it benefits selfish neighbors
540 more than self [46]. Model parameters are in Table S11. We found that both IbMs generated the same
541 qualitative outcomes, where YS won at lower initial density (Fig 5A and 5B), RS won at intermediate
542 initial density (Fig 5E-H) and at even higher initial density, YS won again due to clusters of YS ending up
543 on the biofilm surface by chance and then growing better as clusters of cells which are competing less
544 with each other (Fig 5I-L). This combination of chance events – formation of a small cluster of YS cells
545 at the biofilm surface – with positive feedback became obvious after longer simulations (Fig 5K and
546 5L).

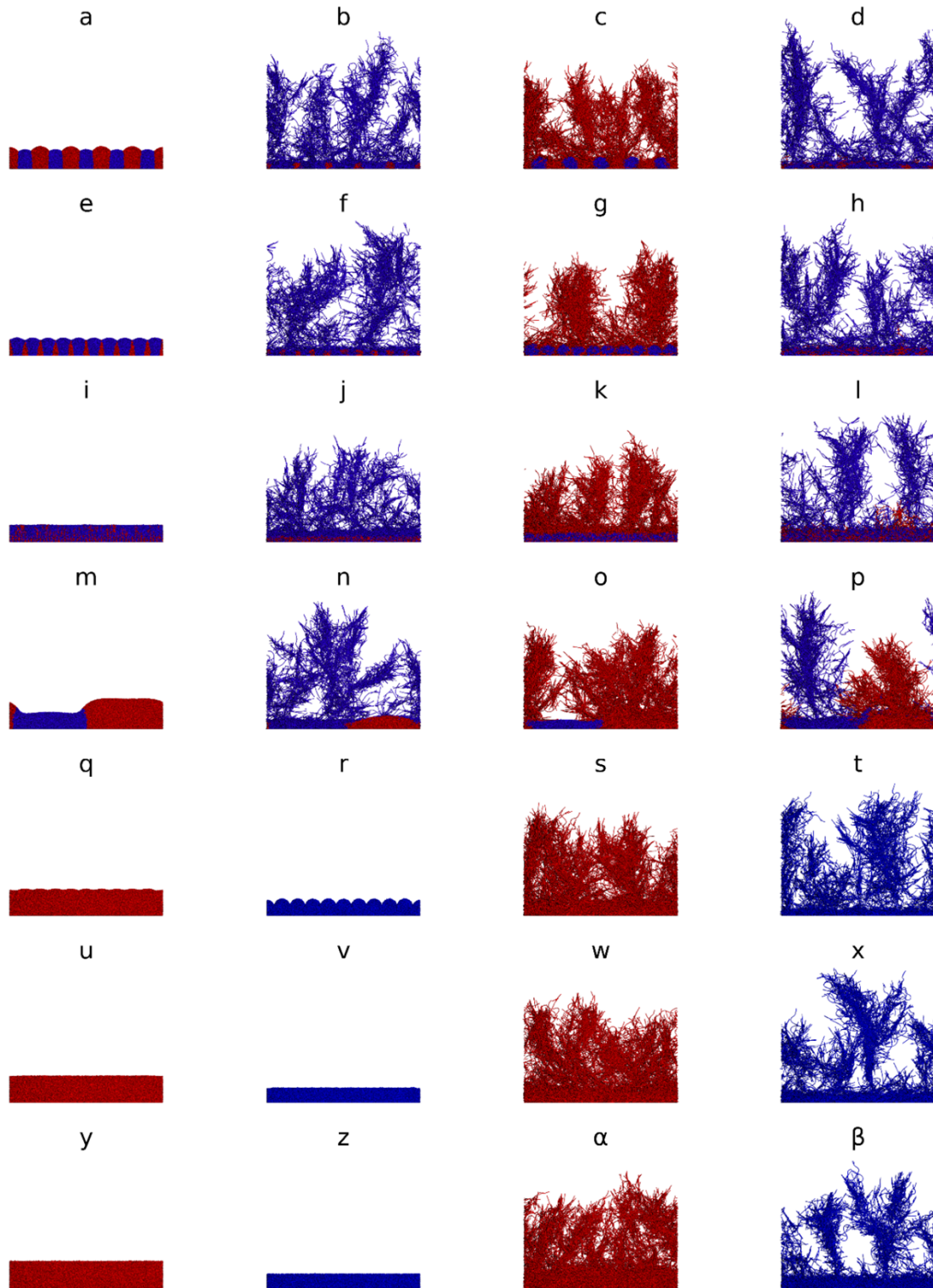
547 While the qualitative outcomes were the same, the initial density thresholds separating regions where
548 different strategies win were somewhat shifted. This was a result of the different biomass spreading
549 algorithms: the shoving in BacSim led to more open spaces and increased mixing of cells locally,
550 compared to force-based mechanical relaxation in iDynoMiCS 2.0, which in this case without EPS
551 production only avoided overlap between agents but did not push cells further away (Fig S6). Note this
552 resulted in increased overall biofilm density in iDynoMiCS 2.0. To compensate for this effect, we had
553 to reduce agent density in iDynoMiCS 2.0 by 47% to maintain similar biofilm densities. Shoving can
554 implicitly model the effect of EPS production generating space between agents, while EPS particles
555 need to be included explicitly to generate space when using FbM simulations. iDynoMiCS 2.0 can do
556 both.



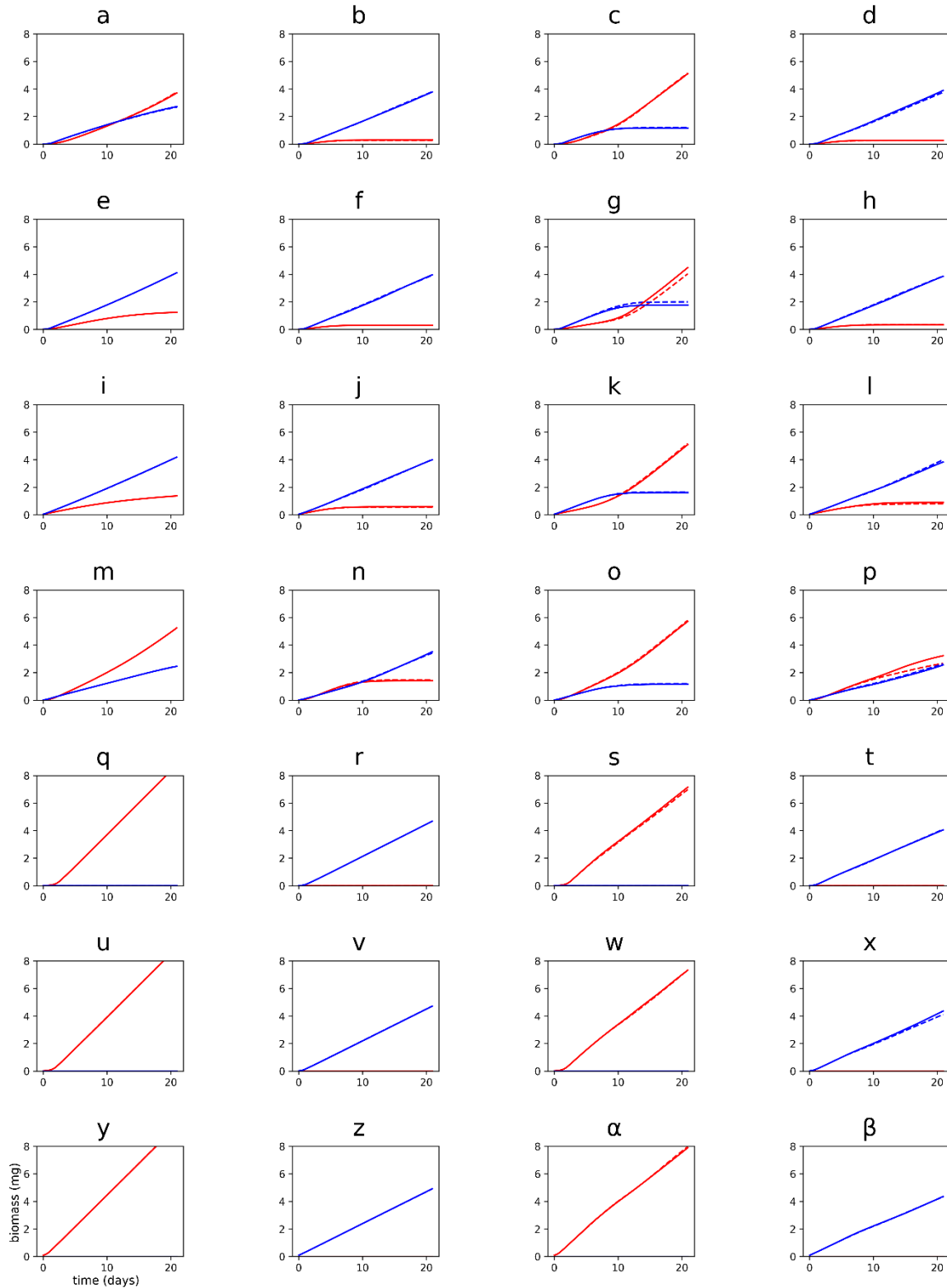
557
 558 **Fig 5. Biofilms promote altruism case study.** Rate Strategist (RS, blue) and Yield Strategist (YS, red)
 559 competitions using the shoving algorithm in BacSim [46] (reproduced from “Kreft J-U (2004). Biofilms
 560 promote altruism. *Microbiology* 150: 2751–2760” with permission) were replicated in iDynoMiCS 2.0
 561 with its force-based mechanics. Cells were initially placed in alternating, equidistant positions with
 562 increasing density from 5 cells per strategy (Scenario 1: a-b), 10 cells each (Scenario 2: e-h) to 50 cells
 563 each (Scenario 3: i-l and c-d). iDynoMiCS 2.0 panels show local oxygen concentration as a linear gray-
 564 level gradient from zero oxygen (0 mg/L, white) to a maximum concentration ($S_{\text{ox_bulk}} = 1$ mg/L, black).
 565 Box 1 shows 3-week-old biofilms. Box 2 zooms into panels i and j. Box 3 shows 10-week-old biofilms
 566 developed from the 3-week-old biofilms shown in the same position on the left.

567 **Filaments outcompeted cocci regardless of growth strategy and RS filaments expanded**
568 **faster**

569 Building on the biofilms promote altruism case study and the capability of iDynamoMiCS 2.0 to simulate
570 spherical, rod-shaped and filamentous microbes, we asked whether filamentous growth provides an
571 additional advantage to Yield Strategists (YS). Since sufficiently large clusters of the cooperative YS cells
572 outcompeted the Rate Strategists (RS) (Fig 5), we reasoned that growing as a filament, which can be
573 considered to be a cluster of cells in one dimension, would give YS an additional advantage. Hence, we
574 competed all combinations in a biofilm setting: coccoid RS vs. coccoid YS, filamentous RS vs coccoid
575 YS, coccoid RS vs. filamentous YS and filamentous RS vs. filamentous YS. As filaments need a larger
576 domain and freedom to bend and spread in all directions, these simulations required a 3D domain of
577 sufficient size. The z-dimension was expanded to 12.5 μm , whilst keeping solute resolution at 1.5625
578 μm . Since the shoving algorithm cannot properly deal with filaments, the FbM of iDynamoMiCS were
579 required. It turned out that filaments were superior to cocci regardless of growth strategy – because
580 filaments quickly gained access to the higher substrate concentrations at the top of the domain where
581 the source of the substrate was located (Fig 6). This range expansion strategy of filaments is similar to
582 cells producing EPS to rise quickly above biofilm neighbors towards the substrate source above, or
583 trees growing faster to the top of the canopy to gain better access to sunlight [47], or the foraging
584 strategy of cord-forming fungi that can form ‘bridges’ between discrete and sparsely scattered patches
585 of nutrient resources [48]. Surprisingly, RS filaments won the competition against YS filaments in each
586 case where the final outcome can be inferred (Fig 6 shows biofilm structures and Fig 7 shows
587 population dynamics over time). A striking difference between Rate Strategist filaments and Yield
588 Strategist filaments is the more open and less dense ‘forest’ structure produced by Rate Strategists.
589 We suggest that the lower substrate consumption rate of the Yield Strategists allows their filaments
590 to grow better in deeper regions of the biofilms than the Rate Strategist filaments, which gain a larger
591 advantage when they happen to grow towards the top. Thus, the stronger competition (or self-
592 inhibition) between Rate Strategist filaments favors expansion over density, leading to a ‘fluffier forest’
593 structure.



594
595 **Fig 6. Filaments rule and gave Rate Strategists an advantage.** Rate Strategists (RS, blue) and Yield
596 Strategists (YS, red) competed in a 3D biofilm domain (200x200x12.5 μm) for 3 weeks. In the first 4
597 rows, strategies competed. Column 1 corresponds to spherical cell scenarios in Fig 2 of Ref [46] but
598 were now simulated in 3D. In column 2, RS formed filaments and in column 3, YS formed filaments.
599 Filaments won regardless of strategy. In column 4, both formed filaments and RS won or likely won.
600 The last 3 rows show single species 'controls' with 10, 20 or 100 initial agents. The first two columns
601 show simulations with spherical YS or RS agents while the last two columns show filament forming YS
602 or RS agents. See Fig 7 for corresponding time courses. Duplicate simulations are shown in Fig S17.



603
604
605
606
607

Fig 7. Growth curves corresponding to competitions of Rate Strategists (RS, blue) and Yield Strategists (YS, red) in Fig 6. Duplicates are plotted with dashed lines. Divergence between replicates is most visible in panels g and p. In panel p, it is too early to definitely call the outcome of competition, but it is likely that RS would win given the biofilm structure after 3 weeks (Fig 6P).

608 Discussion

609 Individual-based models in microbial ecology are uniquely capable of capturing local interactions,
610 individual heterogeneity and adaptation, stochastic processes and emergent properties of biofilms or
611 other spatially structured assemblages [49–58]. The number of publications utilizing IbMs in this field
612 has rapidly increased since the 1990s (S1.13 Fig S10), due to an increased recognition of its potential
613 and facilitated by an increased availability of ready-to-use IbM platforms (discussed below). From its
614 inception, the goal of iDynoMiCS has always been to provide a well-tested, general-purpose platform
615 for individual-based microbial community modeling, enabling users to specify their model in a
616 structured text file rather than requiring them to program, thereby aiding microbial ecology and
617 synthetic biology research, which seeks to reach a mechanistic and predictive understanding of the
618 interactions of natural or synthetic microbes in the environment. The environment for microbes
619 includes engineered reactors and buildings as well as plant and animal hosts. Here, we present
620 iDynoMiCS 2.0, which has been rewritten from scratch to enable flexible agent and process
621 specifications using orthogonal modules called “aspects”, thus removing key limitations of the original
622 iDynoMiCS 1. In addition, we expanded the functionality, most importantly a force-based mechanical
623 interaction framework enabling new agent morphologies such as rods and filaments, a new flexible
624 approach to (bio-)chemical conversions enabling any type of kinetic expression, improvements that
625 make the software easier to use including a GUI, a new protocol and program structure, unit
626 conversions and a large number of efficiency improvements allowing for large scale (10+ million
627 agents) simulations. We have further subjected iDynoMiCS 2.0 to rigorous testing to ensure that the
628 platform and its individual components function correctly. In addition to standard unit tests, we have
629 verified the accuracy of its numerical solvers by using a series of increasingly complex test cases from
630 simpler ones with analytical solutions to more complex ones that have to be compared to independent
631 solvers, culminating in the established Benchmark 3 comparison of nitrifying biofilms with different
632 biofilm modeling approaches and a comparison with prior BacSim simulations of the biofilms promote
633 altruism test case because its positive feedback in the growth of cooperative cell clusters results in
634 higher sensitivity to local cluster formation in biofilms.

635 Biomass spreading mechanisms can affect model outcomes, especially when mixing of different
636 species favors a species that can take advantage of becoming embedded in a cluster of cells of the
637 other species, e.g., if the latter is more rapidly growing towards an energy source. Using nitrifying
638 biofilms, it was previously shown that Cellular Automata (CA) cell division rules led to larger scale
639 stochastic mixing of nitrite oxidizers into the (under specific conditions) more rapidly expanding
640 incomplete ammonia oxidizers than a shoving algorithm that minimized cell-cell overlap, which
641 percolated expansion through the biofilm leading to limited, localized mixing. This resulted in a
642 substantially higher fitness of the nitrite oxidizers in the CA simulations as some of them were ‘going
643 with the flow’ of the ammonia oxidizers towards the oxygen supply [15]. Here, we compared this
644 shoving algorithm with FbM, although using the biofilms promote altruism case study rather than
645 nitrifying biofilms. FbM led to even more limited and localized mixing, producing sharper boundaries
646 between different clusters than shoving (Fig 5). As a result, the chance of clusters of yield strategists
647 to emerge out of clusters of rate strategies (after the latter had overgrown them) and thus eventually
648 winning the competition, was reduced. The biofilm structures resulting from FbM are reminiscent of
649 the smooth, gradual boundaries of biomasses in continuum models of biofilms where biomass
650 spreading is proportional to the pressure gradient [59] (Darcy’s law), but the mixing is more limited
651 with the FbM. Note that continuum models where biomass spreading is driven by density-dependent
652 diffusion can lead to complete mixing if counter-diffusion is not considered and gradual but large-scale
653 mixing if it is [60]. Combining our new results with Kreft et al. (2001) [15], we can rank biomass
654 spreading mechanisms in order of increasing and larger-scale mixing: FbM < shoving < CA. The

655 importance of even subtle differences in biomass spreading mechanisms for biofilm pattern formation
656 and population fitness should become more widely recognized as model predictions can be
657 substantially affected.

658 Morphology matters. There is a great variety of shapes [61] and sizes [62] of microbes while microbes
659 of the same species usually have similar shape and size. Young [63] argued that the variety and
660 uniformity of microbial morphology, the ability of bacteria to actively modify their shapes based on
661 internal or external cues and evolutionary selection towards specific shapes all suggest that bacterial
662 morphology is as important as other traits. Different morphologies may be selected for by different
663 selective pressures and ecological niches such as nutrient limitation, predation, attachment, passive
664 dispersal, active motility and differentiation [63,64]. IbMs have previously been utilized to
665 demonstrate how cell shape can play an important role in spatial organization and evolutionary fitness
666 in biofilms [65,66]. Sphere-shaped, rod-shaped and filamentous microbes are commonly found and
667 can already be modeled with iDynaMiCS 2.0 and the implemented ball-spring approach facilitates
668 future extensions to branching filaments or other morphologies.

669 Filaments win. Our filament case study utilized FbM to simulate filaments consisting of sphere-shaped
670 agents and demonstrated that filamentous growth can provide a strong competitive advantage under
671 nutrient limiting conditions (Fig 6). The advantage derives from the ability of filaments to focus the
672 growth of biomass into one direction rather than merely producing offspring adding to an existing heap
673 of cells. This way, longer distances can be covered and new, nutrient rich territories colonized. This is
674 similar to the strategy of cord-forming fungi who can quickly grow towards new resource hotspots
675 [48,67] and microbes that push themselves towards the nutrient source by producing copious amounts
676 of low-density EPS [47]. The advantage of clusters of yield strategists, who compete less and grow
677 faster than a cluster of rate strategists (of the same size and at the same flux of resources into the
678 cluster), turned into a disadvantage as rate strategists who have reached the top of the biofilm where
679 substrate flux was highest experienced stronger positive feedback than yield strategists. This suggests
680 that filamentous growth is a strategy to escape competition between siblings. Given the huge
681 advantage of filamentous growth found here, the question why filamentous growth is not more
682 common in bacteria arises. It is certainly common in fungi and in the ecologically similar streptomycete
683 bacteria, probably because of improved foraging for scattered patches of resources separated by
684 terrain low in suitable resources like oases in a desert. Also in stream biofilms, filament or chain
685 formation as employed by *Diatoma* spp. enhances nutrient access [29]. Gradient microbes such as
686 *Beggiatoa* spp. or the intriguing cable bacteria [68] form filaments because they need to access
687 electrons from a reduced sediment and electron acceptors from the oxidized water layer above the
688 sediment. Filamentous bacteria are also found in activated sludge flocs in wastewater treatment,
689 where they have the advantage of growing out of the floc into the nutrient richer bulk liquid but are
690 selected against at the settling stage where only fast sinking sludge flocs are recirculated into the
691 activated sludge stage [69,70]. But what are the disadvantages of filaments? Depending on the
692 environment, several disadvantages may arise. Filaments are not only more exposed to beneficial
693 resources but also mechanical or physiological stresses and attack by phages or predators, although
694 some predators may be deterred from grazing larger cells [63]. Further, packaging biomass into smaller
695 propagules is advantageous for dispersal. Filaments also forsake the advantages of motility [63,71].
696 Cell size is also an important factor for pathogenesis, some bacteria may avoid forming filaments to
697 prevent being killed by the host [64].

698 iDynaMiCS 2.0 is joining an increasing number of individual-based modeling platforms that focus on
699 microbes and can support a range of specific models. These platforms can be roughly divided into two
700 groups, based on their subcellular versus ecological dynamics origin and focus. The former group of

701 platforms comes from systems and synthetic biology and seek to discover how specific microbial
702 community behaviors or phenomena can be achieved through the creation of synthetic microbial
703 communities [72]: CellModeller [73], BSim 2.0 [74] and gro [75]. They can simulate microbial
704 communities made up of rod-shaped microbial agents with specific metabolic, sensing and signaling
705 properties. All three can simulate gene regulatory networks and diffusion of signaling molecules in
706 order to explore and/or design synthetic microbial communities. While gro can only simulate 2D
707 systems, CellModeller can simulate both 2D and 3D systems, while BSim 2.0 can only simulate 3D
708 systems. In models that use these platforms, growth kinetics are typically less important than gene
709 regulation, hence growth is modeled as a simple rate, as in CellModeller, or a rate based on cell length,
710 as in BSim 2.0. However, gro allows growth to be based on Monod kinetics. CellModeller and gro do
711 not include environmental constraints such as physical boundaries, thus simulated microbes tend to
712 grow outwards to form round colonies. BSim 2.0, however, can model physical spaces such as
713 microfluidic chemostats where cells may, e.g., grow and release diffusing signaling molecules.

714 The latter group of platforms originate from larger scale microbial ecology models, primarily for
715 biofilms, which seek to explore population dynamics and ecological and evolutionary processes in
716 biofilms. These include iDynoMiCS [17], Biocellion [76], Simbiotics [77], BacArena [78], NUFEB [21],
717 ACBM [79] and McComedy [23]. They focus on microbial growth and metabolism and mass transport
718 such as diffusion of solutes in order to assess how different growth strategies or metabolic interactions
719 affect the fitness of species growing in a biofilm or impact systems-level outcomes in wastewater
720 treatment systems or bioreactors. iDynoMiCS, NUFEB and Simbiotics can all model growth using
721 equations originating from enzyme kinetics that determine reaction rates from substrate
722 concentrations, such as Monod kinetics. Reaction rates and diffusion are coupled and solved using
723 partial differential equation (PDE) solvers. These solvers are made efficient by taking advantage of a
724 separation of timescales, where, e.g., growth of microbes is on a much slower timescale than diffusion.
725 iDynoMiCS and NUFEB both simulate a diffusion boundary layer - a region around the biofilm in which
726 diffusion dominates the transport of solutes - as distinct from the rest of the spatial domain which is
727 well-mixed.

728 BacArena and ACBM are unique in utilizing flux-balance analysis to estimate the metabolic flux through
729 'individual' grid elements, based on their local solute concentrations. Diffusion is then solved using a
730 partial differential equation (PDE) solver. NUFEB can model agent growth based on thermodynamics,
731 calculating the Gibb's free energy of catabolism [39], which could also be done with iDynoMiCS 2.0 as
732 users can specify any arithmetic function for reaction kinetics. Since BacArena and ACBM have to solve
733 flux-balances, which is computationally demanding, the platforms are more restrictive in terms of
734 model scale. BacArena only models agents in a fixed 2D grid, with one agent per grid cell, like a CA,
735 while ACBM groups agents together when evaluating internal processes. The other biofilm modeling
736 platforms simulate grid-free agents that evaluate internal processes on an individual basis. Agents can
737 excrete small particles representing EPS. NUFEB, Simbiotics iDynoMiCS 2.0 also allow adhesive forces
738 to be modeled. In NUFEB and iDynoMiCS 1, agents are spherical, while in Simbiotics, ACBM or
739 iDynoMiCS 2.0, they can be spherical or rod-shaped.

740 Some of the models can simulate fluid motion or advection in addition to diffusion. CellModeller
741 implements an implicit advection model which imposes a linear bulk flow in a given direction. NUFEB
742 can simulate computationally demanding fluid dynamics explicitly through coupling with the fluid
743 dynamics toolbox OpenFOAM, which can solve the fluid velocities based on the biofilm geometry (one
744 way coupling). Forces are then applied to agents based on these flow velocities.

745 The suitability of different individual-based modeling platforms depends on the needs of the user. For
746 exploring synthetic bacterial communities where gene regulation and signaling circuits are engineered

747 into cells, CellModeller, gro or BSim 2.0 may be the most suitable platforms. When details of
748 intracellular dynamics are less relevant or simply unknown and the focus is on interactions between
749 agents and with the environment, such as in biofilms or other spatially structured habitats where mass
750 transport is crucial, NUFEB and iDynoMiCS 2.0 may be the most suitable systems. iDynoMiCS 2.0 offers
751 a highly modular and customizable modeling platform, with both 2D and 3D compartments, spherical,
752 rod-shaped and filamentous microbial agents, a sophisticated reaction-diffusion system and growth
753 models that can be based on any kind of arithmetic expression including enzyme kinetic and
754 thermodynamic based models. It is more straightforward to specify and implement biology in
755 iDynoMiCS 2.0. One key drawback in comparison to NUFEB is that iDynoMiCS 2.0 currently does not
756 model fluid dynamics or advection, and thus if these are important characteristics of the system one
757 wishes to model, NUFEB may be more suitable. BacArena and ACBM offer flux-balance models for
758 metabolism, but therefore come with other limitations.

759 For specific applications, other Agent-based or related bottom-up modeling platforms are worth
760 considering. IndiMeSH [80] is an IBM platform capable of simulating laboratory models of soil habitats.
761 CHASTE [81], BioDynaMo [22], PhysiCell [82] and compuCell3D [83] have been primarily used for tissue
762 modeling, which could make them applicable to the somewhat similar biofilms. Morpheus [84], like
763 compuCell3D, utilizes a cellular Potts model to model multicellular systems. Further, there are several
764 general purpose AbM libraries or toolkits, which facilitate the programming of a specific model by
765 providing a wide range of common routines so models can be specified with a high-level language
766 tailored for this purpose. These libraries could be suitable for certain microbial community models in
767 addition to various other fields of research. They include NetLogo [85], FLAME [86], Mason [87], Repast
768 symphony [88] and others.

769 iDynoMiCS 2.0 has been developed from scratch because the hierarchical inheritance of agent features
770 in iDynoMiCS 1 prevented the fully flexible pick and mix approach to agent characteristics and
771 processes that was required for further expansion of capabilities. Moreover, iDynoMiCS 2.0 sports
772 several key enhancements, such as the ability to simulate spherical, rod-shaped and filamentous
773 microbes and using Force-based Mechanics for biomass spreading, which we show can have important
774 consequences. It can simulate larger 3D domains due to efficient neighbor searching, a faster
775 converging reaction-diffusion solver and numerous other performance improvements. iDynoMiCS 2.0
776 was designed with both ease of use, from a GUI to unit conversions, and ease of extension in mind,
777 providing a solid and well tested simulation platform for a wide variety of microbial community studies
778 to come. We showcased the simulation of filamentous microbes using the biofilm promotes altruism
779 case study and found that the rate strategists gained a stronger advantage from filamentous growth
780 because their tips can escape from the stronger competition between themselves. This demonstrates
781 just one of many new possibilities of iDynoMiCS 2.0.

782 [Acknowledgements](#)

783 iDynoMiCS has undergone development and testing since 2005 thanks to many researchers in the
784 groups of BFS and JUK and seen improvements by many others. We are grateful to all of them. TF, RJC,
785 KA and JUK would like to thank the United Kingdom National Centre for the Replacement, Refinement
786 & Reduction of Animals in Research (NC3Rs) for funding our development of individual-based modeling
787 platforms for the gut environment (Grants NC/K000683/1 and NC/R001707/1). BJRC and BFS would
788 like to thank the Integrated Water Technology (InWaTech) project, which promotes collaborative
789 research between DTU and KAIST, for funding our work on work on microbial aggregation and granular
790 biofilms. SA was funded by a University of Nottingham Vice Chancellor's Scholarship. The funders had
791 no role in study design, data collection and interpretation, decision to publish, or preparation of the
792 manuscript.

793 [Code availability](#)

794 All source code and data associated with this project is published under the GNU General Public License
795 (GPL) compatible CeCILL license V2 and available as an online repository on
796 <https://github.com/kreft/iDynoMiCS-2>

797 References

- 798 1. Flemming H-C, Wuertz S. Bacteria and archaea on Earth and their abundance in biofilms. *Nat*
799 *Rev Microbiol.* 2019;17: 247–260. doi:10.1038/s41579-019-0158-9
- 800 2. Widder S, Allen RJ, Pfeiffer T, Curtis TP, Wiuf C, Sloan WT, et al. Challenges in microbial ecology:
801 building predictive understanding of community function and dynamics. *ISME J.* 2016;10: 2557–
802 2568. doi:10.1038/ismej.2016.45
- 803 3. Parsek MR, Fuqua C. Biofilms 2003: Emerging Themes and Challenges in Studies of Surface-
804 Associated Microbial Life. *J Bacteriol.* 2004;186: 4427–4440. doi:10.1128/JB.186.14.4427-
805 4440.2004
- 806 4. Becker P, Hufnagle W, Peters G, Herrmann M. Detection of Differential Gene Expression in
807 Biofilm-Forming versus Planktonic Populations of *Staphylococcus aureus* Using Micro-
808 Representational-Difference Analysis. *Appl Environ Microbiol.* 2001;67: 2958–2965.
809 doi:10.1128/AEM.67.7.2958-2965.2001
- 810 5. Ackermann M. Microbial individuality in the natural environment. *ISME J.* 2013;7: 465–467.
811 doi:10.1038/ismej.2012.131
- 812 6. Zimmermann M, Escrig S, Hübschmann T, Kirf MK, Brand A, Inglis RF, et al. Phenotypic
813 heterogeneity in metabolic traits among single cells of a rare bacterial species in its natural
814 environment quantified with a combination of flow cell sorting and NanoSIMS. *Front Microbiol.*
815 2015;06. doi:10.3389/fmicb.2015.00243
- 816 7. Wanner O, Eberl HJ, Morgenroth E, Noguera DR, Picioreanu C, Rittmann BE, et al. *Mathematical*
817 *modeling of biofilms.* London: IWA Publishing; 2006.
- 818 8. Kissel JC, McCarty PL, Street RL. Numerical Simulation of Mixed-Culture Biofilm. *J Environ Eng.*
819 1984;110: 393–411. doi:10.1061/(ASCE)0733-9372(1984)110:2(393)
- 820 9. Wanner O, Gujer W. A multispecies biofilm model. *Biotechnol Bioeng.* 1986;28: 314–328.
821 doi:10.1002/bit.260280304
- 822 10. Rittmann BE, Manem JA. Development and experimental evaluation of a steady state,
823 multispecies biofilm model. *Biotechnol Bioeng.* 1992;39: 914–922.
- 824 11. Dockery J, Klapper I. Finger formation in biofilm layers. *SIAM J Appl Math.* 2001;62: 853–869.
- 825 12. Picioreanu C, van Loosdrecht MCM, Heijnen JJ. Mathematical modeling of biofilm structure
826 with a hybrid differential-discrete cellular automaton approach. *Biotechnol Bioeng.* 1998;58:
827 101–116. doi:10.1002/(SICI)1097-0290(19980405)58:1<101::AID-BIT11>3.0.CO;2-M
- 828 13. van Loosdrecht MCM, Heijnen JJ, Eberl HJ, Kreft JU, Picioreanu C. Mathematical modelling of
829 biofilm structures. *Antonie Van Leeuwenhoek Int J Gen Mol Microbiol.* 2002;81: 245–256.
830 doi:10.1023/A:1020527020464
- 831 14. Hartmann R, Singh PK, Pearce P, Mok R, Song B, Díaz-Pascual F, et al. Emergence of three-
832 dimensional order and structure in growing biofilms. *Nat Phys.* 2019;15: 251–256.
833 doi:10.1038/s41567-018-0356-9
- 834 15. Kreft J-U, Picioreanu C, Wimpenny JWT, van Loosdrecht MCM. Individual-based modelling of
835 biofilms. *Microbiology.* 2001;147: 2897–2912. doi:10.1099/00221287-147-11-2897

- 836 16. Hellweger FL, Fredrick ND, McCarthy MJ, Gardner WS, Wilhelm SW, Paerl HW. Dynamic,
837 mechanistic, molecular-level modeling of cyanobacteria: *Anabaena* and nitrogen interaction.
838 Environ Microbiol. 2016;18: 2721–2731. doi:10.1111/1462-2920.13299
- 839 17. Lardon LA, Merkey BV, Martins S, Dötsch A, Picioreanu C, Kreft J-U, et al. iDynaMiCS: next-
840 generation individual-based modelling of biofilms. Environ Microbiol. 2011;13: 2416–2434.
841 doi:10.1111/j.1462-2920.2011.02414.x
- 842 18. Gorochoowski TE, Matyjaszkiewicz A, Todd T, Oak N, Kowalska K, Reid S, et al. BSim: an agent-
843 based tool for modeling bacterial populations in systems and synthetic biology. PLoS ONE.
844 2012;7: e42790. doi:10.1371/journal.pone.0042790
- 845 19. Jang SS, Oishi KT, Egbert RG, Klavins E. Specification and Simulation of Synthetic Multicelled
846 Behaviors. ACS Synth Biol. 2012;1: 365–374. doi:10.1021/sb300034m
- 847 20. Goñi-Moreno A, Amos M. DiSCUS: A Simulation Platform for Conjugation Computing. In: Calude
848 CS, Dinneen MJ, editors. Unconventional Computation and Natural Computation. Cham:
849 Springer International Publishing; 2015. pp. 181–191. doi:10.1007/978-3-319-21819-9_13
- 850 21. Li B, Taniguchi D, Gedara JP, Gogulancea V, Gonzalez-Cabaleiro R, Chen J, et al. NUFEB: A
851 massively parallel simulator for individual-based modelling of microbial communities. Darling
852 AE, editor. PLOS Comput Biol. 2019;15: e1007125. doi:10.1371/journal.pcbi.1007125
- 853 22. Breitwieser L, Hesam A, De Montigny J, Vavourakis V, Iosif A, Jennings J, et al. BioDynaMo: a
854 modular platform for high-performance agent-based simulation. Wren J, editor. Bioinformatics.
855 2022;38: 453–460. doi:10.1093/bioinformatics/btab649
- 856 23. Bogdanowski A, Banitz T, Muhsal LK, Kost C, Frank K. McComedy: A user-friendly tool for next-
857 generation individual-based modeling of microbial consumer-resource systems. Harcombe WR,
858 editor. PLOS Comput Biol. 2022;18: e1009777. doi:10.1371/journal.pcbi.1009777
- 859 24. Grimm V, Berger U, Bastiansen F, Eliassen S, Ginot V, Giske J, et al. A standard protocol for
860 describing individual-based and agent-based models. Ecol Model. 2006;198: 115–126.
861 doi:10.1016/j.ecolmodel.2006.04.023
- 862 25. Grimm V, Berger U, DeAngelis DL, Polhill J, Giske J, Railsback SF. The ODD protocol: a review
863 and first update. Ecol Model. 2010;221: 2760–2768. doi:10.1016/j.ecolmodel.2010.08.019
- 864 26. Trunk T, S. Khalil H, C. Leo J, Bacterial Cell Surface Group, Section for Genetics and Evolutionary
865 Biology, Department of Biosciences, University of Oslo, Oslo, Norway. Bacterial
866 autoaggregation. AIMS Microbiol. 2018;4: 140–164. doi:10.3934/microbiol.2018.1.140
- 867 27. Clegg RJ, Kreft J-U. Reducing discrepancies between 3D and 2D simulations due to cell packing
868 density. J Theor Biol. 2017;423: 26–30. doi:10.1016/j.jtbi.2017.04.016
- 869 28. Janulevicius A, Van Loosdrecht MC, Simone A, Picioreanu C. Cell Flexibility Affects the
870 Alignment of Model Myxobacteria. Biophys J. 2010;99: 3129–3138.
- 871 29. Celler K, Hödl I, Simone A, Battin TJ, Picioreanu C. A mass-spring model unveils the
872 morphogenesis of phototrophic *Diatoma* biofilms. Sci Rep. 2014;4. doi:10.1038/srep03649

- 873 30. Storck T, Picioreanu C, Viridis B, Batstone DJ. Variable cell morphology approach for Individual-
874 based Modeling of microbial communities. *Biophys J.* 2014;106: 2037–2048.
875 doi:10.1016/j.bpj.2014.03.015
- 876 31. Ericson C. Real-time collision detection. Amsterdam ; Boston: Elsevier; 2005.
- 877 32. Purcell EM. Life at low Reynolds number. *Am J Phys.* 1977;45: 3–11.
- 878 33. Berg HC. Random walks in biology. Princeton: Princeton University Press; 1993.
- 879 34. Palsson E. A three-dimensional model of cell movement in multicellular systems. *Future Gener*
880 *Comput Syst.* 2001;17: 835–852. doi:10.1016/S0167-739X(00)00062-5
- 881 35. Ricardo H. A modern introduction to differential equations. Third edition. London [England] ;
882 San Diego, CA: Academic Press; 2021.
- 883 36. Stevens AB, Hrenya CM. Comparison of soft-sphere models to measurements of collision
884 properties during normal impacts. *Powder Technol.* 2005;154: 99–109.
885 doi:10.1016/j.powtec.2005.04.033
- 886 37. Rittmann BE, McCarty PL. *Environmental Biotechnology: Principles and Applications.* New York,
887 N.Y.: McGraw-Hill Education; 2018.
- 888 38. Heijnen JJ. A new thermodynamically based correlation of chemotropic biomass yields. *Antonie*
889 *Van Leeuwenhoek Int J Gen Mol Microbiol.* 1991;60: 235–256.
- 890 39. Gogulancea V, González-Cabaleiro R, Li B, Taniguchi D, Jayathilake PG, Chen J, et al. Individual
891 Based Model Links Thermodynamics, Chemical Speciation and Environmental Conditions to
892 Microbial Growth. *Front Microbiol.* 2019;10. doi:10.3389/fmicb.2019.01871
- 893 40. Dyke P. *Advanced calculus.* London: Macmillan Press, Ltd.; 1998.
- 894 41. Picioreanu C, van Loosdrecht MCM, Heijnen JJ. Effect of diffusive and convective substrate
895 transport on biofilm structure formation: A two-dimensional modeling study. *Biotechnol*
896 *Bioeng.* 2000;69: 504–515.
- 897 42. Gunawardena J. Time-scale separation – Michaelis and Menten’s old idea, still bearing fruit.
898 *FEBS J.* 2014;281: 473–488. doi:10.1111/febs.12532
- 899 43. Rittmann BE, Schwarz AO, Eberl H, Morgenroth E, Pérez J, Van Loosdrecht MCM, et al. Results
900 from the multi-species Benchmark Problem (BM3) using one-dimensional models. *Water Sci*
901 *Technol.* 2004;49: 163–168.
- 902 44. Noguera DR, Picioreanu C. Results from the multi-species Benchmark Problem 3 (BM3) using
903 two-dimensional models. *Water Sci Technol.* 2004;49: 169–176.
- 904 45. Oyebamiji OK, Wilkinson DJ, Li B, Jayathilake PG, Zuliani P, Curtis TP. Bayesian emulation and
905 calibration of an individual-based model of microbial communities. *J Comput Sci.* 2019;30: 194–
906 208. doi:10.1016/j.jocs.2018.12.007
- 907 46. Kreft J-U. Biofilms promote altruism. *Microbiology.* 2004;150: 2751–2760.
908 doi:10.1099/mic.0.26829-0

- 909 47. Xavier JB, Foster KR. Cooperation and conflict in microbial biofilms. *Proc Natl Acad Sci U S A*.
910 2007;104: 876–881. doi:10.1073/pnas.0607651104
- 911 48. Boddy L. Saprotrophic cord-forming fungi: warfare strategies and other ecological aspects.
912 *Mycol Res*. 1993;97: 641–655. doi:10.1016/S0953-7562(09)80141-X
- 913 49. Nadell CD, Bucci V, Drescher K, Levin SA, Bassler BL, Xavier JB. Cutting through the complexity
914 of cell collectives. *Proc R Soc B*. 2013;280: 20122770–20122770. doi:10.1098/rspb.2012.2770
- 915 50. Horn H, Lackner S. Modeling of Biofilm Systems: A Review. In: Muffler K, Ulber R, editors.
916 *Productive Biofilms*. Springer International Publishing; 2014. pp. 53–76. Available:
917 http://link.springer.com/chapter/10.1007/10_2014_275
- 918 51. Song H-S, Cannon WR, Beliaev AS, Konopka A. Mathematical Modeling of Microbial Community
919 Dynamics: A Methodological Review. *Processes*. 2014;2: 711–752. doi:10.3390/pr2040711
- 920 52. Esser DS, Leveau JHJ, Meyer KM. Modeling microbial growth and dynamics. *Appl Microbiol*
921 *Biotechnol*. 2015; 1–16. doi:10.1007/s00253-015-6877-6
- 922 53. Hellweger FL, Clegg RJ, Clark JR, Plugge CM, Kreft J-U. Advancing microbial sciences by
923 individual-based modelling. *Nat Rev Microbiol*. 2016;14: 461–471.
924 doi:10.1038/nrmicro.2016.62
- 925 54. Gorochofski TE. Agent-based modelling in synthetic biology. Pinheiro VB, editor. *Essays*
926 *Biochem*. 2016;60: 325–336. doi:10.1042/EBC20160037
- 927 55. Mattei MR, Frunzo L, D’Acunto B, Pechaud Y, Pirozzi F, Esposito G. Continuum and discrete
928 approach in modeling biofilm development and structure: a review. *J Math Biol*. 2017; 1–59.
929 doi:10.1007/s00285-017-1165-y
- 930 56. Koshy-Chenthittayil S, Archambault L, Senthilkumar D, Laubenbacher R, Mendes P, Dongari-
931 Bagtzoglou A. Agent Based Models of Polymicrobial Biofilms and the Microbiome—A Review.
932 *Microorganisms*. 2021;9: 417. doi:10.3390/microorganisms9020417
- 933 57. Van Den Berg NI, Machado D, Santos S, Rocha I, Chacón J, Harcombe W, et al. Ecological
934 modelling approaches for predicting emergent properties in microbial communities. *Nat Ecol*
935 *Evol*. 2022;6: 855–865. doi:10.1038/s41559-022-01746-7
- 936 58. Nagarajan K, Ni C, Lu T. Agent-Based Modeling of Microbial Communities. *ACS Synth Biol*.
937 2022;11: 3564–3574. doi:10.1021/acssynbio.2c00411
- 938 59. Alpkvist E, Klapper I. A multidimensional multispecies continuum model for heterogeneous
939 biofilm development. *Bull Math Biol*. 2007;69: 765–789. doi:10.1007/s11538-006-9168-7
- 940 60. Rahman KA, Sudarsan R, Eberl HJ. A mixed-culture biofilm model with cross-diffusion. *Bull Math*
941 *Biol*. 2015;77: 2086–2124. doi:10.1007/s11538-015-0117-1
- 942 61. Angert ER. Alternatives to binary fission in bacteria. *Nat Rev Microbiol*. 2005;3: 214–224.
943 doi:10.1038/nrmicro1096
- 944 62. Schulz HN, Jørgensen BB. Big bacteria. *Annu Rev Microbiol*. 2001;55: 105–137.
945 doi:10.1146/annurev.micro.55.1.105

- 946 63. Young KD. The Selective Value of Bacterial Shape. *Microbiol Mol Biol Rev.* 2006;70: 660–703.
947 doi:10.1128/MMBR.00001-06
- 948 64. Yang DC, Blair KM, Salama NR. Staying in Shape: the Impact of Cell Shape on Bacterial Survival
949 in Diverse Environments. *Microbiol Mol Biol Rev.* 2016;80: 187–203.
950 doi:10.1128/MMBR.00031-15
- 951 65. Winkle JJ, Igoshin OA, Bennett MR, Josić K, Ott W. Modeling mechanical interactions in growing
952 populations of rod-shaped bacteria. *Phys Biol.* 2017;14: 055001. doi:10.1088/1478-
953 3975/aa7bae
- 954 66. Smith WPJ, Davit Y, Osborne JM, Kim W, Foster KR, Pitt-Francis JM. Cell morphology drives
955 spatial patterning in microbial communities. *Proc Natl Acad Sci.* 2017;114: E280–E286.
956 doi:10.1073/pnas.1613007114
- 957 67. Aguilar-Trigueros CA, Boddy L, Rillig MC, Fricker MD. Network traits predict ecological strategies
958 in fungi. *ISME Commun.* 2022;2: 1–11. doi:10.1038/s43705-021-00085-1
- 959 68. Pfeffer C, Larsen S, Song J, Dong M, Besenbacher F, Meyer RL, et al. Filamentous bacteria
960 transport electrons over centimetre distances. *Nature.* 2012;491: 218–221.
961 doi:10.1038/nature11586
- 962 69. Martins AMP, Picioreanu C, Heijnen JJ, van Loosdrecht MCM. Three-dimensional dual-
963 morphotype species Modeling of activated sludge flocs. *Environ Sci Technol.* 2004;38: 5632–
964 5641. doi:10.1021/es0496591
- 965 70. Ofițeru ID, Bellucci M, Picioreanu C, Lavric V, Curtis TP. Multi-scale modelling of bioreactor-
966 separator system for wastewater treatment with two-dimensional activated sludge floc
967 dynamics. *Water Res.* 2014;50: 382–395. doi:10.1016/j.watres.2013.10.053
- 968 71. Mitchell JG. The Energetics and Scaling of Search Strategies in Bacteria. *Am Nat.* 2002;160: 727–
969 740. doi:10.1086/343874
- 970 72. Gorochofski TE, Hauert S, Kreft J-U, Marucci L, Shatil N, Tang T-YD, et al. Toward engineering
971 biosystems with emergent collective functions. *Front Bioeng Biotechnol.* 2020;8: Article 705.
972 doi:10.3389/fbioe.2020.00705
- 973 73. Rudge TJ, Steiner PJ, Phillips A, Haseloff J. Computational modeling of synthetic microbial
974 biofilms. *ACS Synth Biol.* 2012;1: 345–352. doi:10.1021/sb300031n
- 975 74. Matyjaszkiewicz A, Fiore G, Annunziata F, Grierson CS, Savery NJ, Marucci L, et al. BSim 2.0: An
976 Advanced Agent-Based Cell Simulator. *ACS Synth Biol.* 2017;6: 1969–1972.
977 doi:10.1021/acssynbio.7b00121
- 978 75. Gutiérrez M, Gregorio-Godoy P, Pérez del Pulgar G, Muñoz LE, Sáez S, Rodríguez-Patón A. A
979 New Improved and Extended Version of the Multicell Bacterial Simulator gro. *ACS Synth Biol.*
980 2017;6: 1496–1508. doi:10.1021/acssynbio.7b00003
- 981 76. Kang S, Kahan S, McDermott J, Flann N, Shmulevich I. *Biocellion* : accelerating computer
982 simulation of multicellular biological system models. *Bioinformatics.* 2014;30: 3101–3108.
983 doi:10.1093/bioinformatics/btu498

- 984 77. Naylor J, Fellermann H, Ding Y, Mohammed WK, Jakubovics NS, Mukherjee J, et al. Simbiotics: A
985 Multiscale Integrative Platform for 3D Modeling of Bacterial Populations. *ACS Synth Biol.*
986 2017;6: 1194–1210. doi:10.1021/acssynbio.6b00315
- 987 78. Bauer E, Zimmermann J, Baldini F, Thiele I, Kaleta C. BacArena: Individual-based metabolic
988 modeling of heterogeneous microbes in complex communities. *PLOS Comput Biol.* 2017;13:
989 e1005544. doi:10.1371/journal.pcbi.1005544
- 990 79. Karimian E, Motamedian E. ACBM: An Integrated Agent and Constraint Based Modeling
991 Framework for Simulation of Microbial Communities. *Sci Rep.* 2020;10: 8695.
992 doi:10.1038/s41598-020-65659-w
- 993 80. Borer B, Ataman M, Hatzimanikatis V, Or D. Modeling metabolic networks of individual
994 bacterial agents in heterogeneous and dynamic soil habitats (IndiMeSH). *PLOS Comput Biol.*
995 2019;15: e1007127. doi:10.1371/journal.pcbi.1007127
- 996 81. Mirams GR, Arthurs CJ, Bernabeu MO, Bordas R, Cooper J, Corrias A, et al. Chaste: an open
997 source C++ library for computational physiology and biology. *PLoS Comput Biol.* 2013;9:
998 e1002970. doi:10.1371/journal.pcbi.1002970
- 999 82. Ghaffarizadeh A, Heiland R, Friedman SH, Mumenthaler SM, Macklin P. PhysiCell: An open
1000 source physics-based cell simulator for 3-D multicellular systems. Poiset T, editor. *PLOS Comput*
1001 *Biol.* 2018;14: e1005991. doi:10.1371/journal.pcbi.1005991
- 1002 83. Swat MH, Thomas GL, Belmonte JM, Shirinifard A, Hmeljak D, Glazier JA. Multi-Scale Modeling
1003 of Tissues Using CompuCell3D. *Methods in Cell Biology.* Elsevier; 2012. pp. 325–366.
1004 doi:10.1016/B978-0-12-388403-9.00013-8
- 1005 84. Starruß J, De Back W, Bruschi L, Deutsch A. Morpheus: a user-friendly modeling environment for
1006 multiscale and multicellular systems biology. *Bioinformatics.* 2014;30: 1331–1332.
1007 doi:10.1093/bioinformatics/btt772
- 1008 85. Wilensky, U. NetLogo. Center for Connected Learning and Computer-Based Modeling,
1009 Northwestern University, Evanston, IL; 1999. Available: <http://ccl.northwestern.edu/netlogo/>
- 1010 86. Chin L, Worth D, Greenough C, Coakley S, Holcombe M, Gheorghe M. FLAME-II : a redesign of
1011 the flexible large-scale agent-based modelling environment. Rutherford Appleton Lab Tech Rep.
1012 2012.
- 1013 87. Luke S, Cioffi-Revilla C, Panait L, Sullivan K, Balan G. Mason: A multiagent simulation
1014 environment. *Simulation.* 2005;81: 517–527.
- 1015 88. North MJ, Tatara E, Collier NT, Ozik J, others. Visual agent-based model development with
1016 repast simphony. Tech. rep., Argonne National Laboratory; 2007.
- 1017 89. Kreft J-U. Mathematical Modeling of Microbial Ecology: Spatial Dynamics of Interactions in
1018 Biofilms and Guts. In: Jaykus L-A, Wang HH, Schlesinger LS, editors. *Food-Borne Microbes:*
1019 *Shaping the Host Ecosystem.* Washington, DC: ASM Press; 2009. pp. 347–377. Available:
1020 <https://onlinelibrary.wiley.com/doi/abs/10.1128/9781555815479.ch19>
- 1021 90. Hubaux N, Wells G, Morgenroth E. Impact of coexistence of flocs and biofilm on performance of
1022 combined nitrification-anammox granular sludge reactors. *Water Res.* 2015;68: 127–139.
1023 doi:10.1016/j.watres.2014.09.036

- 1024 91. Reichert P. Aquasim: A tool for simulation and data analysis of aquatic systems. *Water Sci*
1025 *Technol.* 1994;30: 21–30.
- 1026 92. Wanner O, Reichert P. Mathematical modeling of mixed-culture biofilm. *Biotechnol Bioeng.*
1027 1996;49: 172–184.
- 1028 93. Reichert P, Wanner O. Movement of solids in biofilms: significance of liquid phase transport.
1029 *Water Sci Technol.* 1997;36: 321–328.
- 1030 94. Morgenroth E, Wilderer PA. Influence of detachment mechanisms on competition in biofilms.
1031 *Water Res.* 2000;34: 417–426. doi:10.1016/S0043-1354(99)00157-8
- 1032 95. Noguera DR, Pizarro GE, Regan JM. Modeling Biofilms. *Microbial Biofilms.* John Wiley & Sons,
1033 Ltd; 2004. pp. 222–249. doi:10.1128/9781555817718.ch13
- 1034 96. Picioreanu C, Kreft J-U, van Loosdrecht MCM. Particle-based multidimensional multispecies
1035 biofilm model. *Appl Environ Microbiol.* 2004;70: 3024–3040. doi:10.1128/AEM.70.5.3024-
1036 3040.2004
- 1037 97. Clarke M, Maddera L, Harris RL, Silverman PM. F-pili dynamics by live-cell imaging. *Proc Natl*
1038 *Acad Sci.* 2008;105: 17978–17981. doi:10.1073/pnas.0806786105
- 1039

1040 [S1: Supporting information for](#)

1041 [Is it selfish to be filamentous in biofilms? Individual-based modeling](#)
1042 [links microbial growth strategies with morphology using the new and](#)
1043 [modular iDynoMiCS 2.0](#)

1044 Bastiaan J R Cockx^{1*}, Tim Foster², Robert J Clegg², Kieran Alden², Sankalp Arya³, Dov J Stekel³, Barth F
1045 Smets¹, Jan-Ulrich Kreft^{2*}

1046 ¹Department of Environmental and Resource Engineering, Technical University of Denmark,
1047 Bygningstorvet, Bygning 115, 2800 Kgs. Lyngby, Denmark

1048 ²Centre for Computational Biology & Institute of Microbiology and Infection & School of Biosciences,
1049 University of Birmingham, Edgbaston, Birmingham, B15 2TT, UK

1050 ³School of Biosciences, University of Nottingham, Sutton Bonington Campus, Loughborough,
1051 Leicestershire, LE12 5RD, UK

1052 *Corresponding authors: Jan-Ulrich Kreft j.kreft@bham.ac.uk, Bastiaan J R Cockx: baco@dtu.dk

1053 [S1.1 Introduction](#)

1054 The supplementary materials provide additional details on the iDynoMiCS 2.0 framework and the
1055 model implementations presented in the main manuscript. This includes a further description of the
1056 framework and detailed descriptions of the case studies with their parameters. Moreover, the model
1057 verification and benchmarking against prior work is presented.

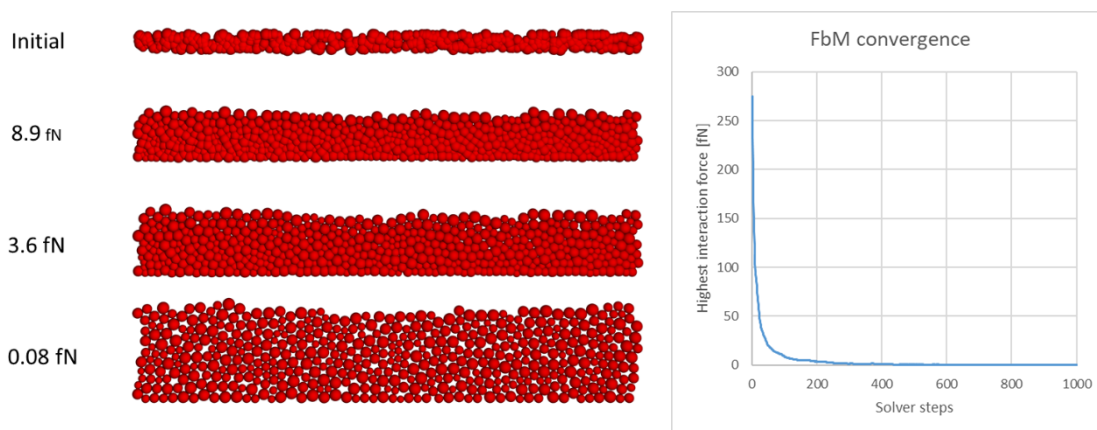
1058 S1.2 Detailed description of Force-based Mechanics (FbM) and testing

1059 The force-based mechanical interactions between agents and agents and surfaces in iDynaMiCS 2.0
1060 rely on both correct detection of overlapping agents or collisions and correct responses. Detection is
1061 simple for stored interactions such as the interaction between the two points of a rod cell connected
1062 by a spring or the interaction between cells in a filament also connected by springs. In this case,
1063 detection is as simple as checking whether interaction data is stored as an aspect of the agent. In the
1064 case of collisions or attractive interactions, collision detection is utilized. Different shapes as well as
1065 periodic boundaries add complexity to this routine. For verification purposes, a total of 36 collision
1066 detection scenarios (Table S1) were tested and included in the software as unit-tests.

1067 **Table S1. In total, 36 collision detection scenarios were included as standard unit tests.** All tests
1068 include two objects to create one of the following scenarios: object-object overlap (hit), no overlap
1069 (miss), overlap through a periodic boundary (periodic hit) and no overlap, but proximity through a
1070 periodic boundary (periodic miss). The sphere and rod objects correspond to agent shapes. Solid
1071 boundaries utilize an (infinite) plane object to allow for agent interactions. The voxel is a cube aligned
1072 with the coordinate grid. Numbers indicate the number of different configurations tested. In all tested
1073 scenarios the collision detection algorithm correctly detected the hits and misses.

	Sphere + Sphere	Sphere + Rod	Rod + Rod	Plane + Sphere	Plane + rod	Voxel + Sphere	Voxel + rod
hit	1	1	1	1	1	1	6
miss	1	1	1	1	1	1	4
periodic hit	1	1	1	1	1	1	3
periodic miss	1	1	1			1	1

1074
1075 Correct interaction response entails relaxing mechanical stresses between agents until a relaxed state
1076 is reached. Criteria for a relaxed state can either be a threshold value for tolerated residual interaction
1077 force in the model state or a threshold value for tolerated agent overlap (μm). In the test in Fig S1, an
1078 over-compressed initial state underwent 1,000 FbM iterations using its default parameters. Initial peak
1079 interaction forces dropped exponentially to asymptotically approach zero (the maximum residual
1080 interaction force (reached after 829 iterations) was less than 0.1 fN).



1081
1082 **Fig S1. FbM led to rapid relaxation of mechanical stress from an initially over-compressed state.** Left
1083 panels from the top showing highest interaction force next to the biofilm structure: 275.1 fN for the
1084 initial state, 8.9 fN after 100 steps, 3.6 fN after 200 steps, 0.08 fN after 1,000 steps. Panel on the right
1085 shows exponential drop of the highest interaction force towards zero, demonstrating convergence of
1086 the FbM solver.

1087 S1.3 Testing Reaction and Diffusion of Chemical Species

1088 In iDynoMiCS 2.0, ODE and PDE solvers are responsible for modeling the diffusion and reaction
1089 (consumption or production) of solutes throughout the simulated system and are therefore
1090 responsible for the maintenance of mass balance within the model. Reactions can be chemical
1091 reactions or catalyzed by individual agents.

1092 To test that these solvers work as intended, a range of test cases were run, which allowed the results
1093 from iDynoMiCS 2.0 to be compared with known analytical solutions. The tests were conducted
1094 starting with the simplest and proceeding to increasingly complex systems. The first two tests were
1095 non-spatial systems, used to test the ODE solver, while the latter two tests were for the more complex
1096 PDE solver in a 2D spatial system. All tests are described in full below.

1097 1. Non-growing Catalyst Agent in a Chemostat

1098 For this simplest test, a single agent was simulated in a chemostat compartment, consuming the
1099 inflowing solute. Fresh medium with a fixed solute concentration flowed into the chemostat at a fixed
1100 flow rate. Spent medium flowed out of the chemostat at a rate equal to the inflow. The consumption
1101 of the solute by the agent was proportional to the solute concentration and to the agent's mass. The
1102 agent was neither growing nor removed.

1103 This system can be described by the following differential equation

$$1104 \quad \frac{dS}{dt} = \frac{QS_0}{V} - \frac{QS}{V} - \frac{mqS}{V}$$

1105 where S is the solute concentration of the substrate in the chemostat, S_0 is the solute concentration in
1106 the inflowing medium, Q is the flow rate with dimension volume per time, V is the volume of the
1107 chemostat, t is time, q is the rate of solute consumption by the agent and m is the mass of the agent.

1108 The steady-state solution for this differential equation is

$$1109 \quad S^* = \frac{QS_0}{Q + mq}$$

1110 This system was simulated in iDynoMiCS 2.0, with timesteps of 100 minutes. The steady state predicted
1111 given parameters in Table S2 was $4.0 \times 10^5 \text{ pg } \mu\text{m}^{-3}$ and the simulated concentration converged to this
1112 steady state exactly (Figure S2A).

1113 **Table S2.** Parameters used in the numerical tests of the chemostat solver.

Parameter	Non-growing agent in chemostat	Growing population in chemostat
S_0	$2.0 \text{ pg } \mu\text{m}^{-3}$	$2.0 \text{ pg } \mu\text{m}^{-3}$
Q	$1.0 \mu\text{m}^3 \text{ min}^{-1}$	$1.0 \mu\text{m}^3 \text{ min}^{-1}$
V	$1.0 \times 10^3 \mu\text{m}^3$	$1.0 \times 10^3 \mu\text{m}^3$
q	$0.1 \mu\text{m}^3 \text{ min}^{-1} \text{ pg}^{-1}$	
K_s		$1.0 \mu\text{m}^3 \text{ min}^{-1} \text{ pg}^{-1}$
m	40 pg	10 pg^*
μ_{max}		0.1 min^{-1}
Y		$0.5 \text{ pg } \text{pg}^{-1}$

1114 *The mass for the simulation of the growing population refers only to the initial mass.

1115 2. Growing Population in a Chemostat

1116 In this simulation, a growing population of agents in a chemostat consumed an inflowing substrate and
1117 converted it to biomass. Outflow removed both spent medium and agents, at a rate equal to the
1118 inflow. Agent removal was stochastic. The agents consumed substrate and grew according to Monod
1119 kinetics:

$$1120 \quad \mu = \frac{\mu_{max} S}{K_S + S}$$

1121 Where μ is the specific growth rate, μ_{max} is the maximum specific growth rate and K_S is the half-
1122 saturation constant, the value of S at which $\mu = \mu_{max}/2$.

1123 Here, the rate of change of substrate concentration is given by

$$1124 \quad \frac{dS}{dt} = \frac{Q S_0}{V} - \frac{Q S}{V} - Y^{-1} \mu(S) P$$

1125 where Y is the biomass yield from the substrate and P is the concentration of the biomass of all
1126 (planktonic) agents in the chemostat, with the rate of change given by

$$1127 \quad \frac{dP}{dt} = - \frac{Q P}{V} + \mu(S) P$$

1128 This system can be solved to find the steady states for both P and S , the washout steady state of $P^* = 0$,
1129 $S^* = S_0$ [89], and the steady with agents present:

$$1130 \quad S^* = \frac{Q/V K_S}{\mu_{max} - Q/V}$$

$$1131 \quad P^* = Y(S_0 - S^*)$$

1132 With the parameter values in Table S2, we obtain the following steady state predictions:

$$1133 \quad S^* = 0.010101 \text{ pg } \mu\text{m}^{-3}$$

$$1134 \quad P^* = 0.994949 \text{ pg } \mu\text{m}^{-3}$$

1135 Running the simulations in iDynoMiCS 2.0 yielded the expected stable steady state (Figure S2B,C). The
1136 mean simulated values at steady state were $S^* = 0.9906 \text{ pg } \mu\text{m}^{-3}$ and $0.0101 \text{ pg } \mu\text{m}^{-3}$. These results
1137 differ from the expected steady states by 0.004% and 0.0003%, respectively.

1138 3. Thin Layer of Non-growing Cells in a Spatial Domain

1139 In this test, a thin non-growing layer of cells, occupying one row of solver grid elements, was simulated
1140 at the bottom of a spatial compartment, with a concentration boundary layer above the cells, and a
1141 well-mixed region above that with the constant concentration of substrate S_0 . Since there was no
1142 gradient of biomass or reaction rates in the horizontal direction, this is effectively a 1D system for
1143 which an analytical solution for the flux, J , can be calculated according to Fick's first law

$$1144 \quad J = D \frac{dS}{dx}$$

1145 where J is the areal flux density through the diffusive region, D is the diffusivity of the solute S and x is
1146 the vertical distance (the direction for the flux and substrate concentration gradient).

1147 Given that at steady state, flux must be constant along the x-axis in the region where the substrate is
 1148 not consumed and then starting to decline where the substrate is consumed by the cells at the bottom,
 1149 we can substitute J by the areal consumption rate at the cell-layer surface. Modeling a simple
 1150 consumption rate proportional to biomass and substrate concentration, we obtain

$$1151 \quad \frac{m q S^*}{A} = D \frac{S_0 - S^*}{\Delta x}$$

1152 where S^* is the steady-state concentration at the biofilm surface, A is the surface area of the biofilm
 1153 and Δx is the depth of the diffusion-dominated boundary layer. This can be rearranged to

$$1154 \quad S^* = \frac{D A S_0}{\Delta x m q + D A}$$

1155 Setting the parameters as shown in Table S3, the predicted steady state concentration at the cell layer
 1156 surface is $S^* = 1.8 \times 10^{-6} pg \mu m^{-3}$. This was matched in the simulation (Figure S2C). Deviations from
 1157 the expected concentration are very small at each height, with the greatest deviation of 0.017% at a
 1158 height of 8 μm .

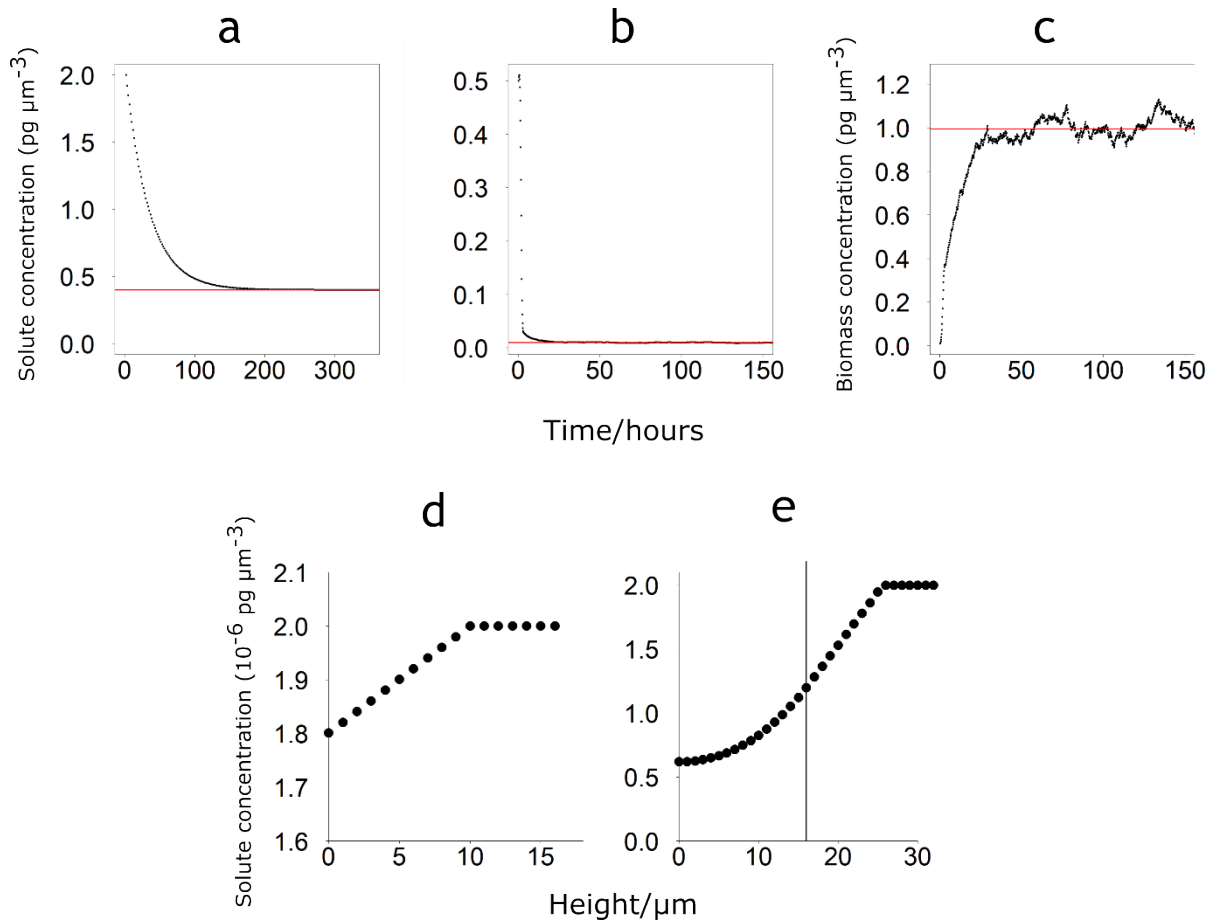
1159 **Table S3.** Parameters used in the numerical tests of the spatial domain in iDynaMiCS 2.0. The total
 1160 biomass was higher for the thick layer, all other parameters were identical.

Parameter	Thin layer	Thick layer (biofilm)
S_0	$2.0 \times 10^{-6} pg \mu m^{-3}$	$2.0 \times 10^{-6} pg \mu m^{-3}$
D	$36,000 \mu m^2 min^{-1}$	$36,000 \mu m^2 min^{-1}$
q	$100 \mu m^3 min^{-1} pg^{-1}$	$100 \mu m^3 min^{-1} pg^{-1}$
m	128 pg	1200 pg
Δx	10 μm	10 μm
A	32 μm^2	32 μm^2

1161

1162 [Biofilm - Thick Layer of Non-Growing Cells in a Spatial Domain](#)

1163 For a biofilm simulation with a thicker layer of cells, no analytical solution is available for the solute
 1164 concentration at the surface of the biofilm. However, the nature of the boundary at the bottom of the
 1165 domain, an inert, solid and flat surface with a no-flux (Neumann) boundary condition, provides another
 1166 testable feature. As a result of the thick biofilm layer consuming substrate while it diffuses towards
 1167 the bottom, the concentration gradient is expected to decrease from the maximum level in the
 1168 diffusion boundary layer to become zero at the inert surface. The results of the test replicated the
 1169 predicted features of the concentration gradient (Figure S2D), suggesting that the diffusion-reaction
 1170 solver and the no-flux boundary conditions in iDynaMiCS 2.0 are functioning as expected. There was
 1171 no horizontal gradient or any unexpected deviations at the horizontal, periodic boundaries.



1172

1173 **Fig S2. Results of numerical tests of the ODE and PDE solvers.** Red lines show expected steady states.
1174 a – Results from the non-growing chemostat population. Concentration tended towards the expected
1175 steady state of $0.4 \text{ pg } \mu\text{m}^{-3}$. b, c – Results from the growing chemostat population. Concentrations
1176 tended towards the expected steady states of $0.0101 \text{ pg } \mu\text{m}^{-3}$ substrate (b) and $0.9949 \text{ pg } \mu\text{m}^{-3}$ biomass
1177 (c). de) – Results from thin cell layer. Concentration at biofilm surface matched predicted
1178 concentration of $1.8 \times 10^{-6} \text{ pg } \mu\text{m}^{-3}$. e – Results from thick cell layer. Vertical line marks biofilm surface.
1179 The substrate concentration gradient was linear in the diffusion boundary layer above the biofilm
1180 surface and then decreased towards zero at the inert boundary at height 0, as expected.

1181 [S1.4 Large scale stress-test](#)

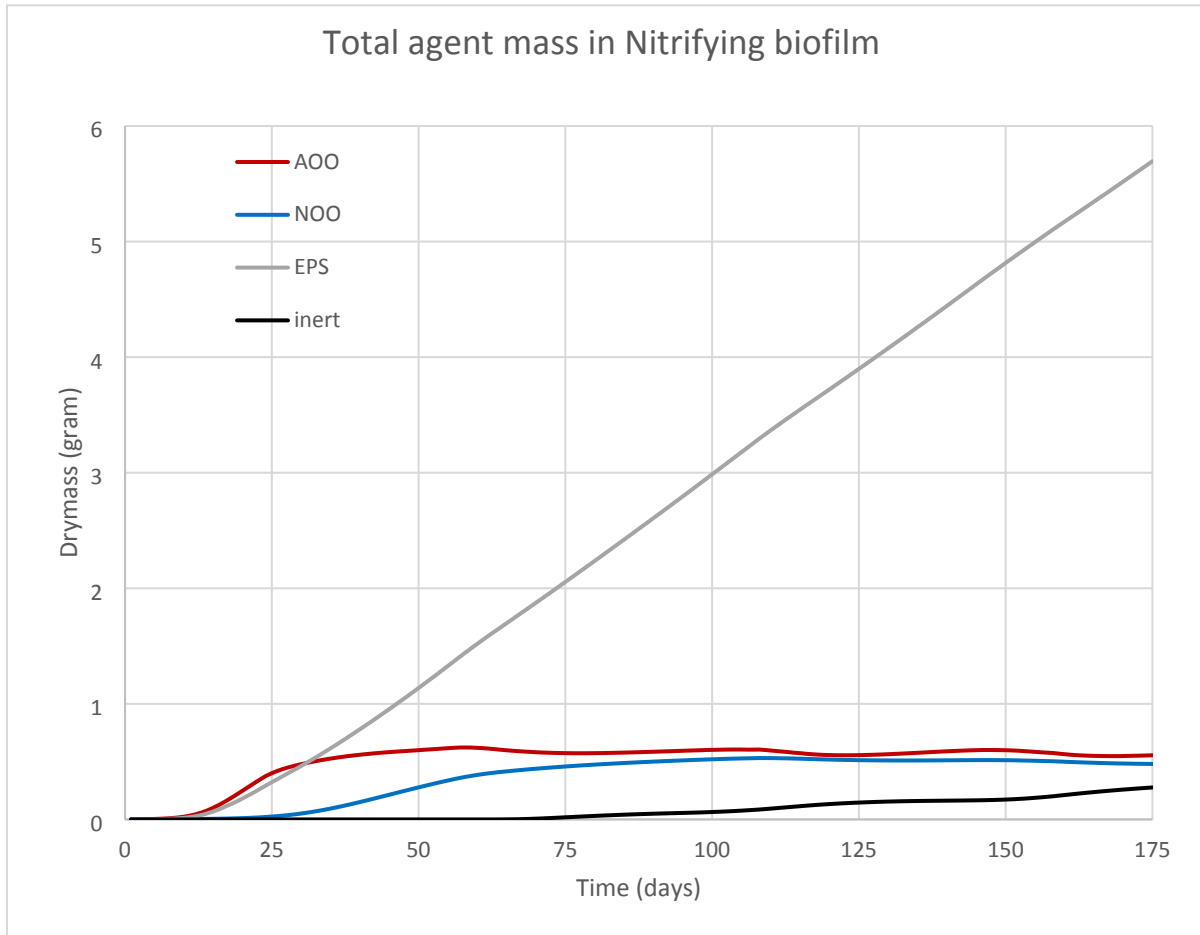
1182 A two-species nitrifying biofilm model was set up to test the ability of iDynoMiCS 2.0 to simulate larger
1183 scale domains. The kinetics are based on Hubaux et al. [90]. A $500 \times 500 \times 500 \text{ } \mu\text{m}$ spatial compartment
1184 with fixed concentrations at the top of the domain was initiated with 1,000 Ammonium Oxidizing
1185 Organisms (AOO) and 1,000 Nitrite Oxidizing Organisms (NOO), randomly distributed over the inert
1186 surface at the bottom of the spatial compartment. Model parameters are given in Table S4 and the
1187 stoichiometry and process kinetics are given in the Petersen matrix in Table S5.

1188 **Table S4. Parameters for the two-species nitrifying biofilm model.** All kinetics for this model are
 1189 based on Hubaux et al. [90].

Ammonium oxidizing organisms (AOO)			
μ_{AOO}	d^{-1}	Maximum specific growth rate of AOO	2.05
Y_{AOO}	$g_{\text{COD}}/g_{\text{N}}$	Growth yield of AOO	0.15
$K_{\text{NH}_4, \text{AOO}}$	$g_{\text{NH}_4\text{-N}}/\text{m}^3$	Half saturation constant for AOO	2.4
$K_{\text{O}_2, \text{AOO}}$	$g_{\text{COD}}/\text{m}^3$	Half saturation constant for AOO	0.6
b_{AOO}	d^{-1}	Decay rate of AOO/End. Resp. rate	0.13
i_{NXB}	$g_{\text{N}}/g_{\text{COD}}$	Nitrogen content in AOO	0.083
Nitrite oxidizing organisms (NOO)			
μ_{NOO}	d^{-1}	Maximum specific growth rate of NOO	1.45
Y_{NOO}	$g_{\text{COD}}/g_{\text{N}}$	Growth yield of NOO	0.041
$K_{\text{O}_2, \text{NOO}}$	$g_{\text{COD}}/\text{m}^3$	Half saturation constant for NOO	2.2
$K_{\text{NO}_2, \text{NOO}}$	$g_{\text{NO}_2\text{-N}}/\text{m}^3$	Half saturation constant for NOO	5.5
b_{NOO}	d^{-1}	Decay rate of NOO	0.06
i_{NXB}	$g_{\text{N}}/g_{\text{COD}}$	Nitrogen content in NOO	0.083

1190 The simulation was run on a single core of an Intel Xeon E5 2660 processor with 256 GB memory, the
 1191 biofilm surpassed 10 million agents after 11 days and 8 hours CPU time, less than the 171 days of
 1192 simulated time of biofilm development. The simulation was stopped after 175 days of simulated time.

1193 The AOO and NOO populations initially grew exponentially as long as growth was not limited by
1194 substrate influx and then grew linearly (Figure S13) while being limited by substrate influx, until
1195 reaching a steady state after around 100 days simulated time due to the balancing of overall growth
1196 and decay rates with only minor fluctuations in population size. There was no decline as bulk
1197 concentrations were kept constant. EPS and inert agents were assumed not to decay in this model,
1198 consequently these agent populations continued to increase.



1199

1200 **Fig S3. Agent mass in the large scale stress test simulation of a biofilm in 3D.** The Autotrophic
1201 nitrifying biofilm was initiated with 1 mg Ammonium Oxidizing Organisms (red) and 1 mg Nitrite
1202 Oxidizing Organisms (blue). Both species produce EPS particles (gray). Agents that drop below 20% of
1203 their division mass as a result of endogenous respiration/decay became inactive (black). The 175-day
1204 biofilm contains 1.02×10^7 agents.

1205 **Table S5: Petersen (stoichiometric) matrix for reactions in the stress test.**

	S_{NH4}	S_{O2}	S_{NO2}	S_{NO3}	X_{AOO}	X_{NOO}	EPS	Kinetic expression
	$gN\ m^{-3}$	$gCOD\ m^{-3}$	$gN\ m^{-3}$	$gN\ m^{-3}$	$gCOD\ m^{-3}$	$gCOD\ m^{-3}$	$gEPS\ m^{-3}$	
AOO growth	$-i_{NXB} - \frac{1}{Y_{AOO}}$	$-\frac{3.43 - Y_{AOO}}{Y_{AOO}}$	$\frac{1}{Y_{AOO}}$		1		$\frac{1}{3}$	$\mu_{AOO} * X_{AOO} * \frac{S}{K_{NH_4, AOO}}$
NOO growth	$-i_{NXB}$	$-\frac{1.14 - Y_{NOO}}{Y_{NOO}}$	$-\frac{1}{Y_{NOO}}$	$\frac{1}{Y_{NOO}}$		1	$\frac{1}{3}$	$\mu_{NOO} * X_{NOO} * \frac{S}{K_{NO_2, NOO}}$
AOO decay					-1			$b_{AOO} * X_{AOO}$
NOO decay						-1		$b_{NOO} * X_{NOO}$

1206

1207 [S1.5 Benchmark 3, a comparison of biofilm modeling platforms](#)

1208 One of the longest established applications of biofilm modeling is modeling the treatment of
1209 wastewater. The International Water Association (IWA) set up a Biofilm Modeling Task group to
1210 compare computational modeling approaches to biofilms and provide guidance for researchers
1211 seeking to simulate biofilms. One of the key outputs of this work was the development of a series of
1212 Benchmark models – biofilm systems that could be modeled in a variety of modeling platforms to
1213 facilitate comparisons between different modeling approaches and establish the effects of different
1214 model designs and simplifying assumptions on simulation outputs [7]. The most complex of a set of
1215 benchmarks, Benchmark 3 (BM3), was designed to simulate microbial competition in a biofilm, with a
1216 source of chemical oxygen demand (COD) being oxidized by a population of heterotrophs and a
1217 population of autotrophs oxidizing ammonia to nitrate. This can be thought of as lumping two-step
1218 nitrification by ammonia- and nitrite-oxidizing organisms into a single process or modeling one-step
1219 nitrification by comammox (complete ammonia oxidizers). BM3 is necessarily limited to what all
1220 models are capable of simulating.

1221 The IWA Biofilm Modeling Task Group ran BM3 simulations on a wide range of modeling platforms,
1222 with a variety of different approaches to modeling biofilms. Later, BM3 was also used for model
1223 validation in the development of iDynoMiCS [17] and NUFEB [21]. Here, iDynoMiCS 2.0 is compared
1224 against a selection of four models from the original IWA task group, as well as NUFEB and iDynoMiCS
1225 1. A summary of the different models and their approaches to BM3 follows:

- 1226 • W – a one-dimensional continuum biomass model run on the AQUASIM software [91] and
1227 developed by Peter Reichert and Oskar Wanner [92,93]
- 1228 • M1 – a variant of the W model with a fixed boundary-layer thickness by Eberhard Morgenroth
1229 et al. [94]
- 1230 • DN – a two-dimensional cellular automaton model developed by Daniel Noguera and
1231 colleagues [95]
- 1232 • CP – a two-dimensional individual-based model, with biomass spreading via shoving,
1233 developed by Cristian Picioreanu and colleagues [96]
- 1234 • NUFEB – A three-dimensional individual-based model that uses a platform derived from a
1235 molecular dynamics simulator by Li et al. [21]
- 1236 • iDynoMiCS 1 – An individual-based model by Lardon et al. [17] used here for 2D simulations.
1237 This platform is the precursor to the one described in this paper, and the implementation of
1238 BM3 is very similar

1239 As this set of modeling platforms represents a variety of different modeling approaches, they provide
1240 a valuable set of results against which to compare iDynoMiCS 2.0. The BM3 scenario has previously
1241 been used by Lardon et al. [17] and Li et al. [21] to benchmark iDynoMiCS 1 and NUFEB, respectively.
1242 Note that NUFEB has also been directly compared with iDynoMiCS 1 based on the BM3 scenario but
1243 varying seven model parameters sampled with a Latin hypercube.

1244 As this set of modeling platforms represents a variety of different modeling approaches, they provide
1245 a valuable set of results against which to compare the results of the BM3 simulation in iDynoMiCS 2.0.
1246 A description of the implementation of the BM3 model in iDynoMiCS 2.0 follows, henceforth referred
1247 to by the abbreviation BM3-iD2.

1248 [BM3-iD2 Model Description](#)

1249 Previous descriptions of BM3 did not explicitly state two critical details that we had to infer by trial and
1250 error. One was that the oxygen concentration in the bulk liquid was kept constant and the other was

1251 that the biomass density of the biofilm had to be tuned by scaling the biomass density of the agents.
 1252 Hence, to facilitate reproduction, we give a full description of BM3 here, using the ODD protocol as a
 1253 framework, with parts of the description that are already covered by the ODD description of iDynoMiCS
 1254 2.0 omitted. The description of BM3-iD2 follows the description of BM3 in Wanner et al. [7].

1255 *Overview*

1256 *Purpose and patterns*

1257 This model simulates multi-species biofilms growing in an aqueous environment as commonly found
 1258 both in nature and in treatment systems for wastewater and drinking water. The biofilm is composed
 1259 of two species representing microbial functional groups – an aerobic heterotroph and an aerobic
 1260 autotrophic nitrifier. Both of these species undergo inactivation processes which transform an agent’s
 1261 active biomass to inert biomass, meaning that there are three types of biomass present in the biofilm:
 1262 heterotrophic, autotrophic and inert. The two microbial species compete for oxygen and for space in
 1263 the biofilm and are transformed into the same inert biomass, leading to vertical stratification of the
 1264 three different types of biomass through the biofilm.

1265 The purpose of the BM3-iD2 model is to allow comparison between iDynoMiCS 2.0 and other biofilm
 1266 models. Previous publications did not report time series and only some reported biomass distributions,
 1267 which limits comparisons to various characteristics of the steady state, including solute concentrations
 1268 in the bulk liquid, biomass concentrations and to some extent biomass distribution. A close match to
 1269 other implementations of BM3 would demonstrate that differences in biomass spreading mechanisms
 1270 between the models have little impact on overall transformation and growth rates in the biofilms and
 1271 suggest that iDynoMiCS 2.0 is a reliable modeling platform. Deviations would suggest that differences
 1272 between models, primarily different biomass spreading mechanisms, could affect predictions of
 1273 overall biofilm performance.

1274 **Table S6. Parameters used in the Benchmark 3 simulations.**

Parameter	Value		
	Standard case	High ammonium	Low ammonium
Ammonium influent concentration	6 g m^{-3}	30 g m^{-3}	1.5 g m^{-3}
Dilution rate	0.0111 min^{-1}		
Volume of bulk liquid	$4.0 \times 10^6 \mu\text{m}^3$		
COD influent concentration	30 g m^{-3}		
Carrier surface area	$320 \mu\text{m}^2$		
Biofilm thickness	$500 \mu\text{m}$		
Constant oxygen concentration in bulk liquid	10 g m^{-3}		
Biofilm density	10 g L^{-1}		
Agent density Shoving	12.5 g L^{-1}		
Agent density FbM	10.08 g L^{-1}		
Agent division dry mass	4 pg		
Boundary layer thickness	$0 \mu\text{m}$		
Shove Factor	1.05		

1275

1276 [Entities, State Variables and Scales](#)

1277 The computational domain for BM3-iD2 is a 2-dimensional, spatially explicit compartment with a width
1278 of 320 μm . As detailed in Submodels, 2D simulations have a virtual third dimension with a thickness of
1279 1 μm , meaning the effective surface area at the base of the biofilm is 320 μm^2 . This domain represents
1280 a vertical slice of a biofilm that contains all simulated microbial agents. In order to maintain the defined
1281 biofilm thickness of 500 μm , all agents with a central point greater than 500 μm above the base are
1282 removed from the simulation at the beginning of each simulated time step. The biofilm compartment
1283 is coupled to a well-mixed bulk liquid compartment with a volume of 0.4 μL , which receives a constant
1284 inflow of 0.26 $\mu\text{L h}^{-1}$, with outflow of the bulk liquid at the same rate. Inflowing bulk liquid contains
1285 three solutes at fixed concentrations: organic carbon measured as chemical oxygen demand (COD) at
1286 30 g m^{-3} , oxygen at 10 g m^{-3} and ammonium at three different concentrations (Table S6). Solute are
1287 well-mixed in the bulk compartment and in the upper portion of the spatial domain above the
1288 boundary layer. In the portion of the spatial domain that contains the boundary layer and biofilm,
1289 solutes diffuse through a grid with a resolution of 20 μm . The principal agents in BM3-iD2 are the
1290 microbial agents, of which there are two types – autotrophs and heterotrophs. Both species are
1291 modeled as spherical cells (coccioids), with a division mass of 4 pg. Agent biomass is composed of active
1292 and inert portions for both species.

1293 Most models in the original IWA task group could directly set a biofilm biomass density as a parameter,
1294 and this is defined in BM3 as 10 g L^{-1} . However, as iDynoMiCS-2 is an individual-based model, users can
1295 only set the density of agents, with biofilm density an emergent property. In order to match the biofilm
1296 density in other models, simulations were run with a variety of agent densities until a biofilm density
1297 matching the other models was obtained. Since the emergent biofilm density depended on the agent
1298 relaxation method used, in simulations using shoving, an agent (cellular) biomass density of 12.5 g L^{-1}
1299 was used, while in simulations using Force-based Mechanics, an agent biomass density of 10.08 g L^{-1}
1300 was used. It was also discovered that the biofilm density used when running BM3 in the original
1301 iDynoMiCS 1 was incorrectly stated in the publication [17] as an agent biomass density of 15 g L^{-1} , but
1302 this led to a final biofilm density of $\sim 12 \text{ g L}^{-1}$. Hence these simulations were rerun with the modified
1303 agent density used in BM3-iD2 to match a biofilm density of 10 g L^{-1} . These new results in iDynoMiCS
1304 1 are also presented here.

1305 [Process Overview and Scheduling](#)

1306 The BM3-iD2 simulation proceeds in global timesteps representing 12 minutes of simulated time.
1307 Within this timestep, various core processes are simulated in a set order, while other processes
1308 (specifically, data reporting processes) occur less regularly than the global timestep. The order of
1309 processes in the spatial domain is as follows:

- 1310 1. Agent removal – Agents with centers higher than 500 μm above the base of the biofilm are
1311 removed
- 1312 2. Mechanical relaxation – Either shoving or Force-based Mechanical relaxation to minimize
1313 agent overlaps
- 1314 3. Reaction-diffusion – Agents determine their reaction rates, based on solute concentrations
1315 and biomass amounts. Active agents also grow and divide. Solute concentration grids are
1316 updated according to reaction rates, and the boundary with the bulk compartment is updated
1317 (see *Submodels*)
- 1318 4. Reporting (only every 2 simulated hours) – Biomass density grids and totals of different
1319 biomasses are written to files

1320 In the bulk compartment, there is a simpler series of processes as follows:

- 1321 1. Solute concentrations are updated according to inflows, outflows and diffusion into the biofilm
 1322 (as determined by the boundary between the two compartments)
 1323 2. A file recording solute concentrations is updated.
 1324 These two sets of processes are carried out separately within each timestep, with the bulk
 1325 compartment carrying out its processes before the biofilm compartment.

1326 Design Concepts

1327 The majority of the design concepts in BM3-iD2 are identical to the design concepts of the modeling
 1328 platform itself, iDynaMiCS 2.0. Therefore, for a fuller description of the design concepts, see the
 1329 Methods section of this paper. Design concepts that are specific to the BM3-iD2 model are described
 1330 below.

1331 *Emergence:* The interactions between the two species, especially the competition for oxygen and for
 1332 space, because the top of the biofilm is maintained at a constant height, lead to particular distributions
 1333 of biomass within the biofilm, which in turn determine the steady state concentrations of COD and
 1334 ammonium in the bulk liquid.

1335 *Interaction:* Agents interact with one another and with solutes in their local environment. Physical
 1336 interactions cause agents to push against one another as they grow, causing a flow of actively growing
 1337 agents and their neighbors upwards towards the top of the biofilm. Consumption of solutes by agents
 1338 determines the rates of solute diffusion into the biofilm and also facilitates competition between
 1339 agents, with agents near the top of the biofilm having access to solutes at greater concentrations.

1340 iDynaMiCS 2.0 has two main agent overlap relaxation methods: A Shoving algorithm and Force-based
 1341 Mechanics, described in detail in *Submodels*. In order to establish whether these different relaxation
 1342 methods affected the results of BM3, simulations were run with both methods, with agent density
 1343 adjusted for each method, to achieve an overall biofilm density of 10 g L⁻¹.

1344 **Table S7. Petersen (stoichiometric) matrix for reactions in the Benchmark 3 simulations**, adapted
 1345 from Rittmann [43] and Lardon et al. [17]. Biomasses are denoted with X. Specifically, X_H = heterotroph
 1346 active biomass, X_N = nitrifier (autotroph) active biomass. Substrate concentrations are denoted with S,
 1347 S_S for the organic substrate COD, S_N for ammonium and S_{O2} for oxygen. For descriptions of the other
 1348 parameters, see Table S8.

	Biomass type		Substrate			Kinetic expression
	Active	Inert	S _S	S _N	S _{O2}	
Heterotroph growth	1		$\frac{-1}{Y_H}$		$\frac{-(1 - Y_H)}{Y_H}$	$\mu_{max,H} \frac{S_S}{K_S + S_S} \frac{S_{O_2}}{K_{O_2,H} + S_{O_2}} X_H$
Heterotroph decay	-1	1				$b_{in,H} X_H$
Heterotroph maintenance	-1				-1	$b_{res,H} X_H \frac{S_{O_2}}{K_{O_2,H} + S_{O_2}}$
Autotroph growth	1			$\frac{-1}{Y_H}$	$\frac{-(4.57 - Y_N)}{Y_N}$	$\mu_{max,N} \frac{S_N}{K_N + S_N} \frac{S_{O_2}}{K_{O_2,N} + S_{O_2}} X_N$
Autotroph decay	-1	1				$b_{in,N} X_N$
Autotroph maintenance	-1				-1	$b_{res,N} X_N \frac{S_{O_2}}{K_{O_2,N} + S_{O_2}}$

1349

1350 **Initialization**

1351 50 agents of each species are placed randomly within the bottom 160 μm of the spatial compartment
 1352 before the first timestep of the simulation. Each of these agents starts with 10 pg active biomass,
 1353 meaning they are expected to divide in the first timestep as the division mass is 4 pg, introducing some
 1354 stochastic variation in total agent masses. Initial solute concentrations are set to the values in the bulk
 1355 inflow.

1356 **Submodels**

1357 **Bulk solute dynamics**

1358 The concentrations of COD and ammonium are solved in the bulk compartment according to Equation
 1359 3. However, the concentration of oxygen in the bulk had to be fixed at 10 g m^{-3} to match the results
 1360 reported for BM3. In the well-mixed region of the spatial compartment that does not contain any
 1361 agents, concentrations are set to those in the bulk compartment. In the rest of the spatial domain,
 1362 solutes diffuse through the solute grid and are consumed by agents at rates according to the agent
 1363 reactions.

1364 **Table S8. Kinetic parameters in the Benchmark 3 models.**

Parameter	Symbol	Value
Maximum specific growth rate, heterotroph	$\mu_{\text{max,H}}$	5.9976 day^{-1}
Half-saturation constant, heterotroph growth	K_S	4 g m^{-3}
Heterotroph growth yield	Y_H	0.63
Half-saturation constant, heterotroph maintenance	$K_{\text{O}_2,\text{H}}$	0.2 g m^{-3}
Maintenance rate, heterotroph	$b_{\text{res,H}}$	0.32 day^{-1}
Decay rate, heterotroph	$b_{\text{ina,H}}$	0.08 day^{-1}
Maximum specific growth rate, autotroph	$u_{\text{max,N}}$	0.1386 day^{-1}
Half-saturation constant, autotroph growth	K_N	1.5 g m^{-3}
Autotroph growth yield	Y_N	0.063
Maintenance rate, autotroph	$b_{\text{res,N}}$	0.12 day^{-1}
Decay rate, autotroph	$b_{\text{ina,N}}$	0.03 day^{-1}
Half-saturation constant, autotroph maintenance	$K_{\text{O}_2,\text{N}}$	0.5 g m^{-3}

1365

1366 **Agent Reactions**

1367 Both species carry out three different reactions, a metabolism reaction, a maintenance reaction and
 1368 an inactivation reaction. The metabolism reaction is equivalent to growth, increasing biomass, and
 1369 using COD as electron donor and oxygen as electron acceptor in the case of heterotrophs and
 1370 ammonium as electron donor and oxygen as electron acceptor in the case of autotrophs. The
 1371 maintenance reaction represents the endogenous respiratory consumption of biomass for cell
 1372 maintenance and oxidizes biomass with oxygen. The inactivation reaction lumps any additional loss of
 1373 active biomass into a single decay process which converts metabolically active biomass to inert
 1374 biomass. The growth and respiration reactions proceed according to Monod kinetics, while the
 1375 inactivation reaction is governed by first order kinetics. See Tables S7 for the Petersen matrix and S8
 1376 for the kinetic parameters.

1377 BM3-iD2 Results

1378 Once parameters were finalized, three replicates of each combination of case and relaxation method
1379 were simulated in iDynoMiCS 2.0 for 120 simulated days. Additionally, three replicates of each case
1380 were simulated in iDynoMiCS 1 with the newly adjusted agent density parameter for the purposes of
1381 comparison. Solute concentrations generally reached steady state within 20 simulated days, while
1382 biomass took longer to reach steady state (Figure S4). To compare iDynoMiCS 2.0 to the other models
1383 that have run BM3, various output variables were compared (Figures S4, S5, Table S9). These included
1384 steady state concentrations of COD and ammonium, steady state densities of the various biomass
1385 forms and the distribution of biomass within the biofilm.

1386 *Solute Concentrations*

1387 Unsurprisingly, the BM3 results from iDynoMiCS 1 and iDynoMiCS 2.0 were very similar (Figure S4).
1388 These models have very similar basic designs and in a simple biofilm model, behave very similarly.
1389 Furthermore, there is no clear impact of the biomass spreading mechanism used in iDynoMiCS 2.0 as
1390 the Shoving or Force-based Mechanics simulation results were very similar. However, different agent
1391 densities were required for these two spreading methods to produce an overall biofilm density of 10
1392 g L⁻¹, because the FbM produced denser biofilms than the Shoving algorithm in the absence of this
1393 adjustment. This is because Shoving is generally used to model the effect of EPS production – increased
1394 distance between cells – implicitly by using a Shoving factor, a multiplier on the radius of the cells.
1395 There is no EPS in BM3, including EPS would reduce biofilm density in a mechanistic way.

1396 Steady state bulk liquid concentrations from the results with Shoving were compared with the results
1397 from the other models using the multivariate version of the t-test, Hotelling's 1-sample T² test. In the
1398 case of results from simulations with the Shoving relaxation algorithm, results from iDynoMiCS 2.0 did
1399 not differ significantly from the distribution of the other models (Table S9). Despite this, the steady
1400 state COD concentrations in iDynoMiCS 1 and 2.0 were generally higher than those in the other models
1401 (Figure S4, Table S9). In simulations using Force-based mechanics, there was a significant difference
1402 between iDynoMiCS 2.0 and the other models in the high ammonium case (Figure S9). This suggests
1403 that using force-based mechanics leads to a more pronounced difference in the BM3 results, due to
1404 differences in the spreading and distribution of biomass.

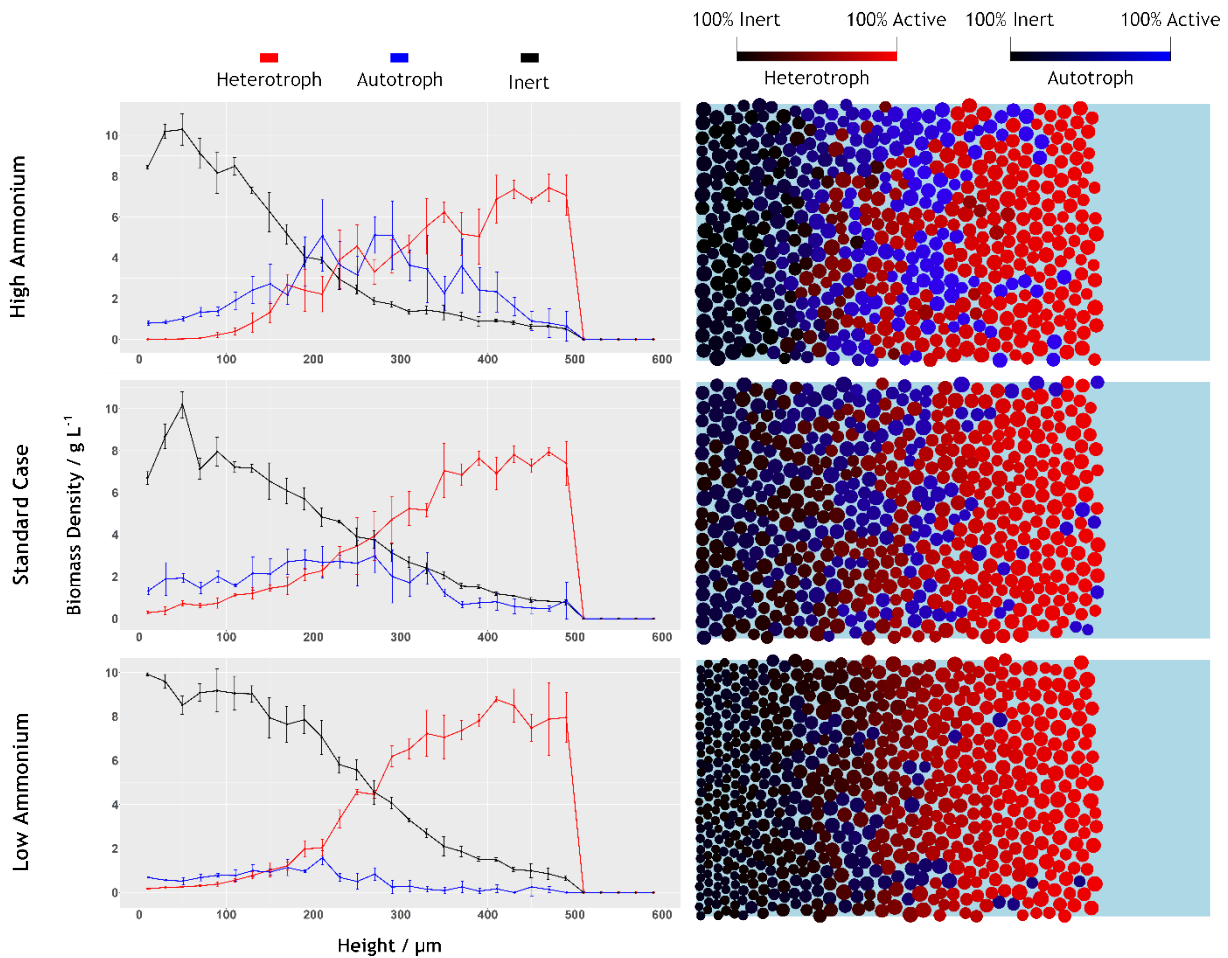
1405 *Biomass distribution*

1406 Another key output of the BM3-iD2 model is the biomass density and vertical distribution. As both
1407 species in the model can have both active and inert biomass, there are three different biomass types
1408 with different concentrations and distributions - heterotrophic, autotrophic and inert. The total areal
1409 densities of these biomass types are compared between models in Table S10. Vertical distributions of
1410 the various biomass types in the different cases are shown in Figure S6. These show a qualitatively
1411 similar pattern to the CP model [44], with fast-growing heterotrophs dominating the top of the biofilm,
1412 while autotrophs grow more slowly and are at their most abundant in the middle or bottom of the
1413 biofilm. Autotrophs vary widely in abundance between the different cases, being at very low numbers
1414 in the low ammonium case. This is to be expected, given that their energy source is at a low
1415 concentration. In all three cases, the bottom of the biofilm is dominated by inert biomass due to the
1416 lower substrate concentrations at the bottom of the biofilm reducing growth relative to maintenance
1417 and inactivation. This is most pronounced in the low ammonium case, which has the highest proportion
1418 of inert biomass of the three cases.

1419 Given the differences in modeling approaches of the various IWA task group models, one might expect
1420 iDynoMiCS 1 and iDynoMiCS 2.0 to produce results closer to the NUFEB and CP models than to any of
1421 the other IWA task group models. Although, the NUFEB results were close, differences with CP are
1422 larger. In fact, the results from the W platform were the closest match in steady state solute

1423 concentrations, while those from the M1 platform were the closest match for overall biomass
1424 densities. This is particularly interesting given that these are both 1-dimensional platforms utilizing the
1425 AQUASIM software rather than agent-based. It is possible that the similarity derives from a closer
1426 match in biomass distribution than with the other models due to less stochastic mixing of the biomass.
1427 However, as the biomass distributions were not published for these models, this is difficult to
1428 determine. Hotellings 1-sample T^2 tests were carried out to compare the areal biomass densities in
1429 iDynoMiCS 2.0 to that in the IWA models. The results from iDynoMiCS 2.0 do not differ significantly
1430 from the set of results from the IWA models.

1431

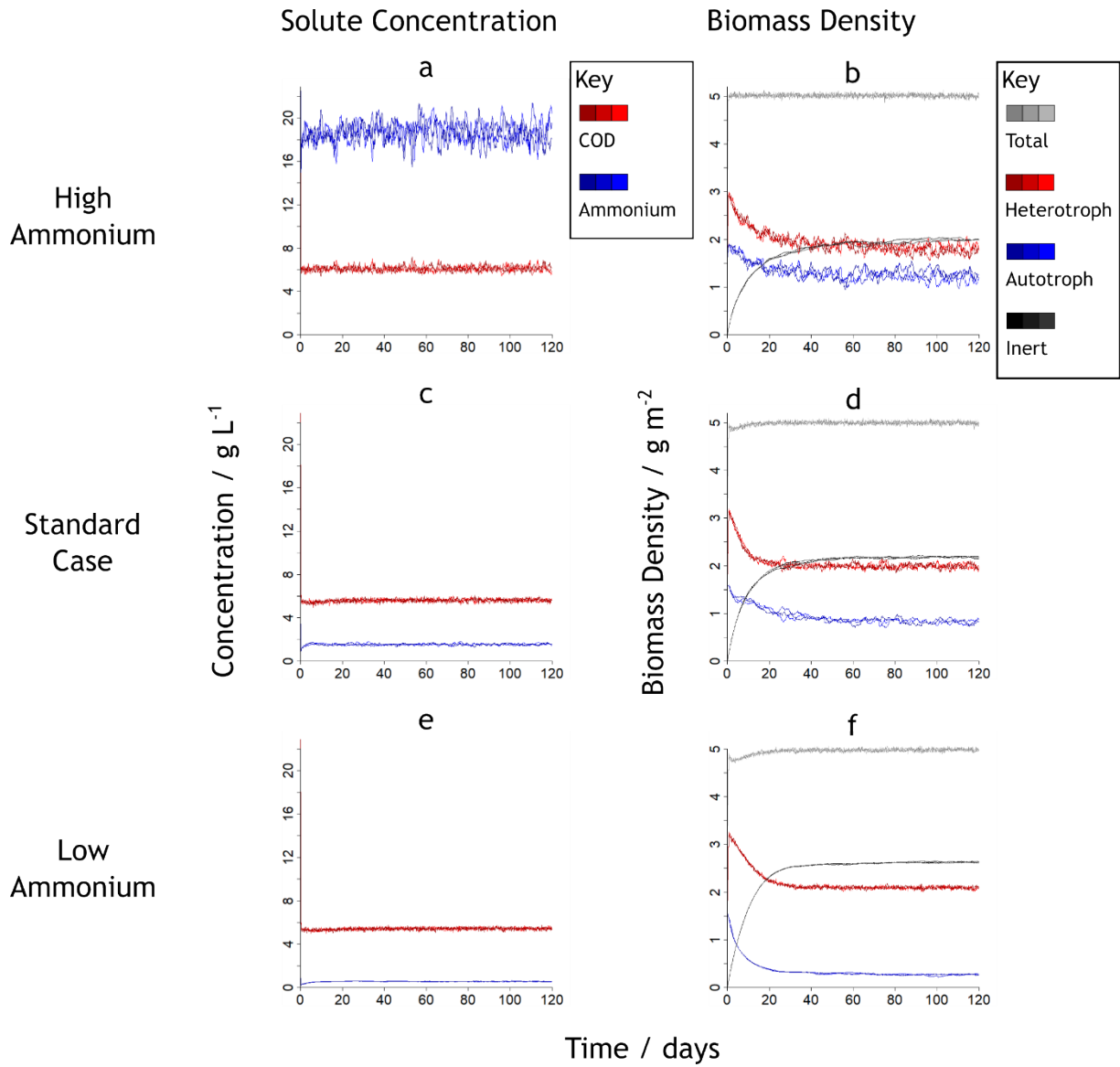


1432

1433

1434 **Fig S4. BM3-iD2 biomass distribution in the three cases.** Left column shows the average areal density
1435 of each biomass type. Error bars show the standard deviation based on the three replicates run for
1436 each case. Right column shows an example from the final timestep of one replicate for each case.
1437 Coloring of agents shows the proportion of biomass that is active or inert.

1438



1439

1440 **Fig S5. BM3-iD2 solute concentrations and areal biomass densities over time in the three simulated**
1441 **cases.** Lines of different shades of the same color represent different replicates of the simulations run
1442 with different random number seeds. Three replicates were run for each case. Results are from the
1443 simulations with the Shoving biomass spreading algorithm.

1444 **Table S9. Steady state substrate concentrations in the various IWA task group models and in**
 1445 **iDynoMiCS 1 and iDynoMiCS 2.0.** Results for the latter models were averaged over the stochastic
 1446 steady states. Hotelling's T² tests were performed to compare the results from iDynoMiCS 2.0 to those
 1447 from all other models, including the IWA models, NUFEB and iDynoMiCS 1.

		High ammonium		Standard case		Low ammonium	
		COD	Ammonium	COD	Ammonium	COD	Ammonium
IWA models	CP	5.45	18.15	5.14	1.50	4.39	0.44
	DN	5.56	20.26	5.14	1.74	4.98	0.48
	W	5.86	18.93	5.39	1.59	5.19	0.48
	M1	5.35	17.03	4.84	1.45	4.66	0.45
NUFEB		5.74	18.42	5.21	1.72	5.18	0.53
iDynoMiCS models	iDynoMiCS 1	6.08	18.58	5.63	1.55	5.45	0.55
	iDynoMiCS 2.0 (Shoving)	6.11	18.68	5.62	1.54	5.43	0.54
	Hotelling's T ² Test p-value	0.0548		0.0523		0.1306	
	iDynoMiCS 2.0 (FbM)	6.13	18.50	5.60	1.55	5.41	0.55
	Hotelling's T ² Test p-value	0.0431		0.0646		0.0765	

1448

1449 **Table S10. Steady state areal biomass density** (mass per unit surface area) of different types of
 1450 biomass in the biofilm. The iDynoMiCS 2.0 results are from simulations using the Shoving algorithm.
 1451 Hotelling's T² tests were performed to compare the results from iDynoMiCS 2.0 to those from the IWA
 1452 models. Biomass density was not reported on the NUFEB model benchmark, and it is thus not included
 1453 in this comparison.

		Areal biomass density (g/m²)		
		Heterotroph	Autotroph	Inert
High ammonium	CP	1.71	1.07	2.42
	DN	2.92	1.10	0.98
	W	1.73	1.07	2.20
	M1	1.83	1.24	1.93
	iDynoMiCS 2.0	1.76	1.24	2.00
	Hotelling's T ² Test p-value	0.6016		
Standard Case	CP	1.81	0.72	2.60
	DN	2.88	0.68	1.44
	W	1.88	0.79	2.33
	M1	2.02	0.83	2.15
	iDynoMiCS 2.0	1.94	0.86	2.17
	Hotelling's T ² Test p-value	0.5475		
Low ammonium	CP	2.11	0.23	2.73
	DN	2.96	0.13	1.91
	W	2.00	0.21	2.80
	M1	2.14	0.21	2.65
	iDynoMiCS 2.0	2.08	0.26	2.62
	Hotelling's T ² Test p-value	0.1038		

1454

1455 S1.6 Supplementary Information for “Comparing the effect of different biomass
1456 spreading mechanisms: Biofilms promote altruism case study”

1457 **Table S11. Model parameters for 3D simulations of the “biofilms promote altruism” case study**

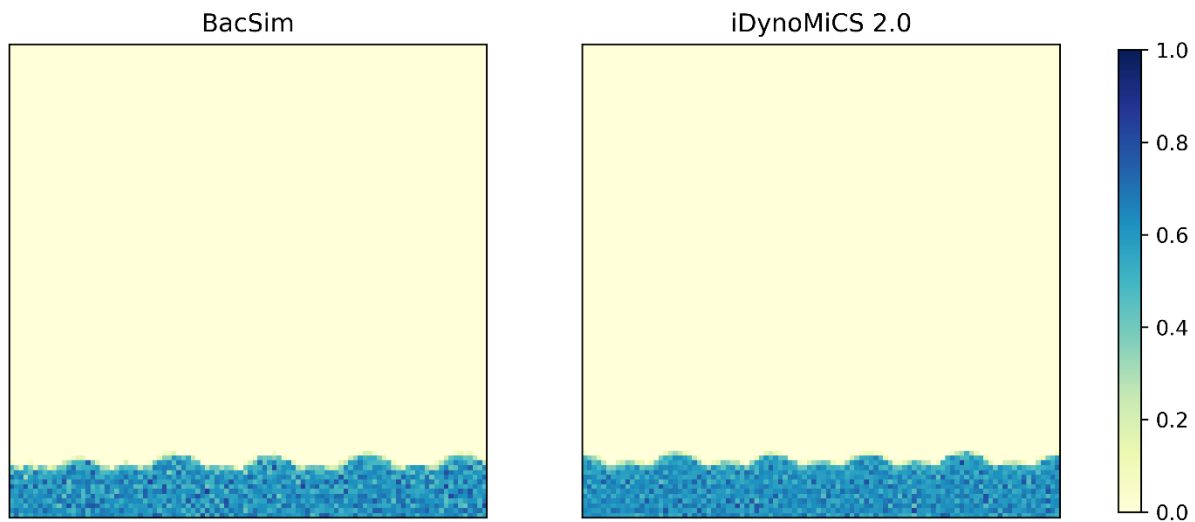
Description	Symbol	Value	Unit	Reference/notes
<i>Global timestep</i>	Δt	1	hour	Kreft 2004
<i>Total simulation</i>	t_{\max}	21	day	Kreft 2004
Coccoloid				
<i>Agent density</i>	ρ_x	0.1363	pg/fL	Adjusted to match biofilm density (original 0.29 pg/fl)
<i>Division threshold</i>	x_{\max}	0.08	pg	Chosen, 0.08 pg as this results in approximately the same cell volume used in BacSim
Filament				
<i>Agent density</i>	ρ_x	0.1363	pg/fL	Chosen
<i>Division threshold</i>	x_{\max}	0.14	pg	Chosen
<i>Transition threshold</i>	$x_{\text{transition}}$	0.09	pg	Chosen
<i>Spine stiffness</i>	k_{spine}	0.56	fN	Chosen
<i>Rod radius</i>	r_{rod}	0.37	μm	Chosen
<i>Connecting spring stiffness</i>	k_{connect}	0.2778	fN	Chosen
<i>Torsion spring stiffness</i>	k_{torsion}	0.2778	fN	Chosen
<i>Detachment probability</i>	$P(\text{detach})$	0.1		Chosen
Yield strategist				
Kox	K_{ox}	0.3	mg/L	Kreft 2004
Vmax	V_{\max}	0.55836	1/h	
<i>Biomass per reaction</i>	Y_x	0.147	gX/gN	Kreft 2004
<i>Oxygen per reaction</i>	Y_{ox}	-3.19565	gOx/gN	Kreft 2004
Rate strategist				
Kox	K_{ox}	0.6	mg/L	Kreft 2004
Vmax	V_{\max}	2.23344	1/h	
<i>Biomass per reaction</i>	Y_x	0.0735	gX/gN	Kreft 2004
<i>Oxygen per reaction</i>	Y_{ox}	-3.19565	gOx/gN	Kreft 2004
Domain				
<i>Length x</i>	l_x	200	μm	Kreft 2004
<i>Length y</i>	l_y	200	μm	Kreft 2004
<i>Length z</i>	l_z	12.5	μm	Chosen (original 2 μm)
<i>Distance between solute nodes</i>	res	25/16	μm	Chosen (original 2 μm)
<i>Diffusion boundary layer</i>	$l_{\text{diffusion}}$	40	μm	Kreft 2004
Solutes				
<i>Initial oxygen concentration</i>	$S_{\text{ox_init}}$	1	mg/L	Kreft 2004
<i>Oxygen diffusivity</i>	D_{ox}	2.00E-05	cm^2/s	Kreft 2004
Chemostat				
<i>Volume</i>	$V_{\text{chemostat}}$	1	mm^3	Chosen
<i>Flowrate</i>	$Q_{\text{chemostat}}$	0.06	mm^3/h	Chosen

1459 Shoving as used in BacSim results in more open space between agents compared to mechanical
1460 relaxation as used in iDynoMiCS 2.0, which by default only resolves overlap between agents. To
1461 compensate for this effect, we have reduced agent density in iDynoMiCS 2.0 by 53%, such that overall
1462 biofilm densities remain similar. In order to compare biofilm densities, the computational domain was
1463 split into 100x100 bins. Each bin receives a number equal to the total mass of all agents with their
1464 center of gravity in the bin, division by the bin volume reveals the local biofilm density (Fig S6).

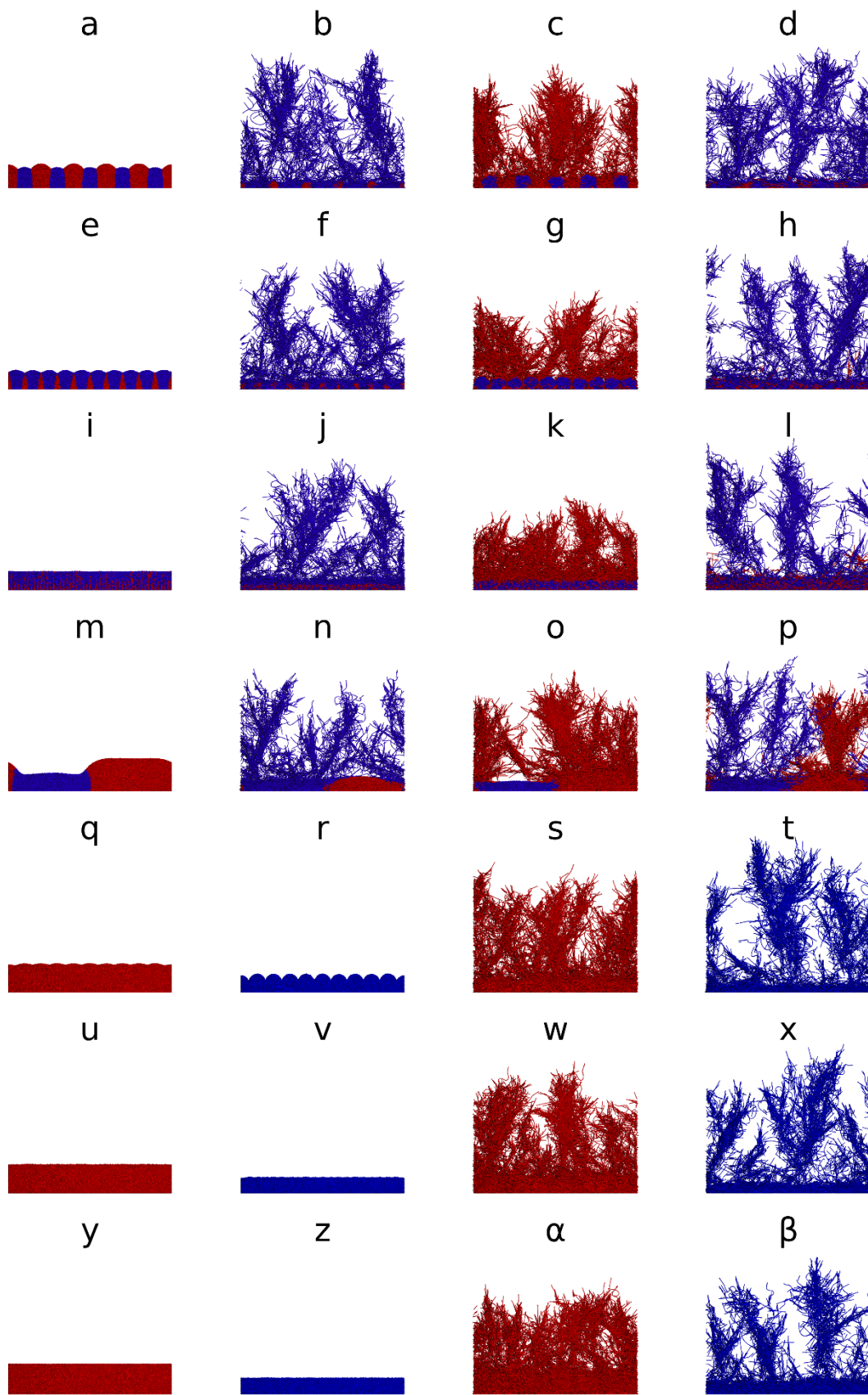
1465 For both the iDynoMiCS 2.0 and BacSim simulations, inspection of biofilm density at different heights
1466 revealed that the majority of bin rows were not significantly different in terms of density in comparison
1467 to the total amount of filled bins. For both platforms we observed a significant drop-off of biofilm
1468 density at the top surface where bins may be partially filled and the expansion front may result in a
1469 sparser local agent population.

1470 In BacSim simulations we observe a significant biofilm density drop in the first row of bins (at the base
1471 of the biofilm). This may be a result of how the BacSim shoving algorithm resolves interactions with a
1472 hard surface in combination with less efficient sphere packing at a flat surface. No significant biofilm
1473 density drop was observed at the base of the iDynoMiCS 2.0 simulations. With both platforms,
1474 occasional small but significant peaks or drops in biofilm density ($2.5 < P < 5.0$) are observed in some
1475 bins. These occasional drops and peaks are likely artifacts as a result of a spatial aliasing effect between
1476 the binning resolution and local sphere packing.

1477 With both platforms, density bins, excluding bins at the biofilm extremes, follow a normal distribution.
1478 After the before mentioned agent density adjustment, no significant difference in the overall biofilm
1479 density is observed between simulations of the two platforms. The standard deviation of density bins
1480 is higher in BacSim simulations. This can be explained by the difference in agent properties, maximum
1481 agent size is kept the same in iDynoMiCS 2.0, translating into a higher overall amount of agents with a
1482 lower mass, resulting in less bin-to-bin mass fluctuation.



1483 **Fig S6. Comparison of agent density ($\text{pg}/\mu\text{m}^3$) distributions in biofilms simulated in BacSim using the**
1484 **shoving algorithm vs iDynoMiCS 2.0 using FbM.** The panels correspond to Fig 5A (left) and B (right).
1485 The computational domain was split into 100x100 grid elements, each received the full mass of agents
1486 whose center of gravity was inside the grid element, division by the grid element volume gave the local
1487 biofilm density ($\text{pg}/\mu\text{m}^3$). iDynoMiCS 2.0 agent density was reduced by 53% in order to achieve a similar
1488 overall biofilm density. With BacSim the biofilm density at the base was observed to be significantly
1489 lower than in the rest of the biofilm. The BacSim simulations further showed a higher standard
1490 deviation amongst bins, due to the higher agent density in these simulations.
1491



1492

1493 **Fig S7. Replicates of biofilms promote altruism case study simulations shown in Fig. 6.**

1494 **S1.7 Model initiation**

1495 **Box S1. Example of a simple iDynoMiCS 2.0 protocol file used to specify a particular model to be**
1496 **read and executed by the platform.**

```
<?xml version="1.0" encoding="UTF-8"?>
<document>
<simulation name="simple_biofilm" outputfolder="../results" log="NORMAL">
  <timer stepSize="3 [h]" endOfSimulation="10 [d]" />
  <speciesLib>
    <species name="bacterium">
      <speciesModule name="coccooid" />
      <aspect name="reactions" class="InstantiableList">
        <list nodeLabel="reaction" entryClass="RegularReaction">
          <reaction name="growth">
            <expression value="mass*mumax*(carbon/(carbon+Ks))*((oxygen/(oxygen+Kox)))">
              <constant name="Ks" value="2.4[g/m+3]" />
              <constant name="Kox" value="0.6[g/m+3]" />
              <constant name="mumax" value="2.05[d-1]" />
            </expression>
            <stoichiometric component="mass" coefficient="1.0" />
            <stoichiometric component="oxygen" coefficient="-18.0" />
            <stoichiometric component="carbon" coefficient="-4.2" />
          </reaction>
        </list>
      </aspect>
    </species>
    <species name="coccooid">
      <aspect name="density" class="Double" value="0.15" />
      <aspect name="surfaces" class="AgentSurfaces" />
      <aspect name="morphology" class="String" value="coccooid" />
      <aspect name="volume" class="SimpleVolumeState" />
      <aspect name="radius" class="CylinderRadius" />
      <aspect name="divide" class="CoccooidDivision" />
      <aspect name="divisionMass" class="Double" value="0.2 [pg]" />
      <aspect name="updateBody" class="UpdateBody" />
    </species>
  </speciesLib>
  <compartment name="biofilm-compartment">
    <shape class="Rectangle" resolutionCalculator="MgFASResolution" nodeSystem="true">
      <dimension name="X" isCyclic="true" targetResolution="2.0" max="32.0"/>
      <dimension name="Y" isCyclic="false" targetResolution="2.0" max="64.0">
        <boundary extreme="1" class="FixedBoundary" layerThickness="32.0">
          <solute name="carbon" concentration="1.0 [mg/l]" />
          <solute name="oxygen" concentration="8.74 [mg/l]" />
        </boundary>
      </dimension>
    </shape>
    <solutes>
      <solute name="carbon" concentration="1.0 [mg/l]" defaultDiffusivity="2000.0 [um+2/s]" biofilmDiffusivity="1500.0 [um+2/s]" />
      <solute name="oxygen" concentration="8.74 [mg/l]" defaultDiffusivity="2000.0 [um+2/s]" biofilmDiffusivity="1500.0 [um+2/s]" />
    </solutes>
    <spawn class="randomSpawner" domain="32.0, 1.0" priority="0" number="30" morphology="COCCOID">
      <templateAgent>
        <aspect name="species" class="String" value="bacterium" />
        <aspect name="mass" class="Double" value="0.2" />
      </templateAgent>
    </spawn>
    <processManagers>
      <process name="agentRelax" class="AgentRelaxation" priority="0" />
      <process name="PDEWrapper" class="PDEWrapper" priority="1" />
    </processManagers>
  </compartment>
</simulation>
</document>
```

1497

1498 [S1.8 Software structure](#)

1499 **Box S2. This example shows how with a few lines of code a new aspect class can be created.** In this
1500 case it is a class that calculates a coccooid radius from its volume. Because here the abstract super class
1501 “Calculated” is extended, the newly written class integrates seamlessly in the framework as
1502 initialization and data handling is handled automatically.

```
Import ...  
/** Example of a basic calculated aspect that returns the radius of a coccooid agent in 3D */  
public class SimpleCoccooidRadius extends Calculated {  
    public Object get( AspectInterface agent ) {  
        return ExtraMath.cubeRoot( agent.getDouble( AspectRef.agentVolume ) * 0.75 / Math.PI );  
    }  
}}
```

1503

1504 [S1.9 Included test scenarios](#)

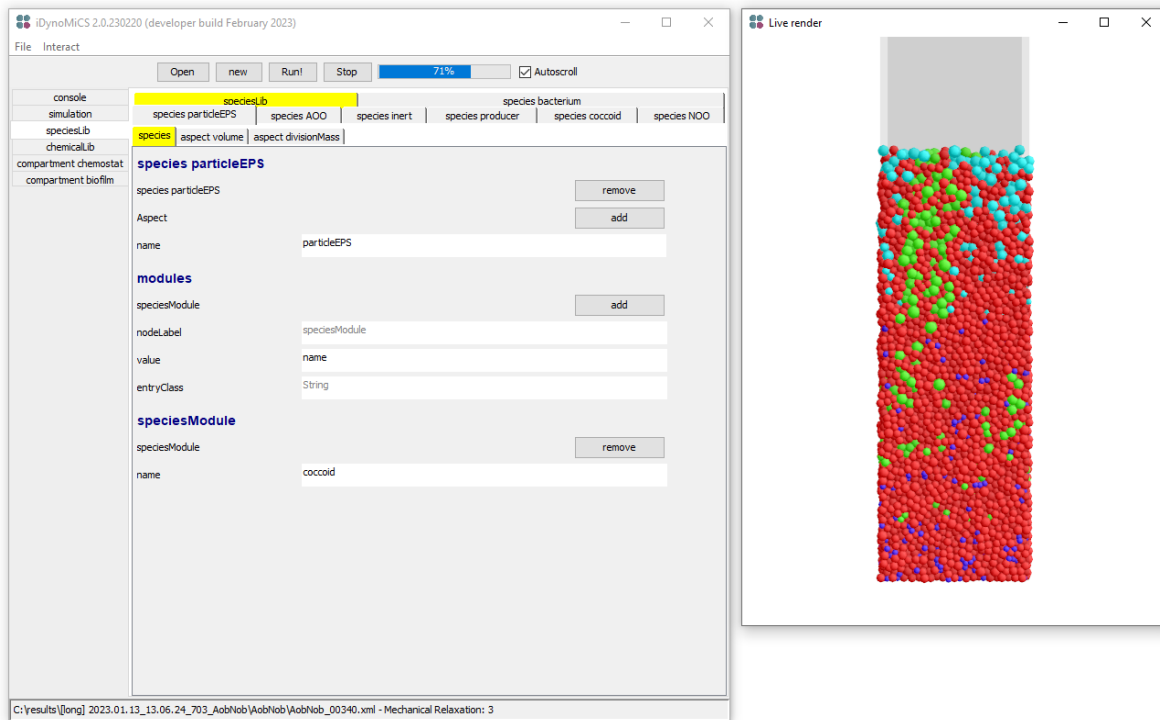
1505 **Table S12 A selection of test protocols that are included with iDynoMiCS 2.0.**

Title	File	Description
Simple	simple.xml	Minimalistic protocol file testing basic functionality with default parameters.
Chemostat	chemostat.xml	A basic chemostat setup with a reaction occurring in the environment (non-agent mediated).
Fed-batch	fedbatch.xml	Basic fedbatch scenario, agents grow in a non-spatial compartment with constant “feed” increasing volume and supplying solutes.
Sensing	simple_sensing.xml	Basic scenario with local solute sensing, agents “differentiate” when the signal surpasses a threshold concentration.
Conditional colouring	conditional_colouring.xml	A basic nitrifying biofilm with conditional coloring, agents receive a color gradient based on the amount of internally stored eps.
Bacilli	bacilli.xml	A basic setup with 2 colonies of rod shaped agents merging.
Plasmid spatial	plasmid.xml	A basic setup testing plasmid transfer in a spatial compartment.
Plasmid chemostat	plasmid_chemostat.xml	A basic setup testing plasmid transfer in a well-mixed environment.
Stress test	stress_test_7c.xml	A large scale nitrifying biofilm used to test the limits of iDynoMiCS 2.0.
Benchmark 3	/BM3/ (6 files)	A set of model scenarios corresponding the 3 different ammonium concentrations as analog to the benchmark 3 cases using FbM or shoving.
Altruism 2.5D	c10_ld_fb.xml, d10_ld_fb.xml, e10_ld_fb.xml	A set of model scenarios corresponding to those found in “Biofilms promote altruism” Kreft 2004, Fig 4. scenario c, d and e.
Altruism 3D	/altruism 3D/ (28 files)	A set of model scenarios corresponding to scenarios presented in Fig 6.
Reaction diffusion tests	/reaction diffusion/ (4 files)	A set of model scenarios corresponding to the reaction and diffusion tests as presented in S1.3
Unit tests	/unit-tests/ (7 files)	A set of protocols used for automated software and solver testing.

1506

1507 S1.10 The graphical user interface

1508



1509

1510 **Fig S8. Preview of the iDynaMiCS 2.0 GUI during simulation.** The GUI may be used to review, edit or
1511 create protocol files before running them. During the simulation, the simulation state may be viewed
1512 but no longer edited (left). The GUI can further provide useful feedback including key information
1513 such as substrate concentration, species abundance, convergence of the reaction diffusion solver,
1514 etc. through the console. Spatial compartments can be rendered directly to provide insights in agent
1515 species distribution and concentration gradients (right). Lastly the GUI can be used to extract key
1516 data from iDynaMiCS 2.0 output files, convert between EXI and XML files and convert numbers
1517 between different unit systems including SI and iDynaMiCS 2.0 base units.

1518 S1.11 Plasmid Dynamics

1519 For plasmid dynamics, two distinct processes were implemented: conjugative transfer from donor to
1520 recipient cells and loss of the plasmid due to segregation. Plasmid loss can only happen upon cell
1521 division and hence was encoded as a probability. Conjugation was considered pili-driven, with a
1522 maximum length pili can reach before they start retracting. The dynamics of transfer were
1523 incorporated based on the live cell imaging by Clarke *et al.* (2008) [97].

1524 From the imaging, certain aspects of F-pilus extension and retraction can be observed: During
1525 extension, the filament elongates from the base. A fully extended 4- μm pilus retracts completely. F-
1526 pili on the same cell are independently regulated, with about three pili growing and retracting
1527 asynchronously. The average time required for extension and retraction of the pili informed the
1528 extension and retraction speeds of the pili used in the plasmid dynamics process manager.

1529 In the model, the conjugation process begins with pili extension, assuming pili extend in all directions
1530 from the cell surface. On encountering a recipient, the pilus tries to attach to its surface and if a pilus
1531 attaches to a recipient cell, all pili start retracting. Certain pili are capable of transferring the plasmid
1532 without pili retraction, but others transfer the plasmid only upon cell surface to surface contact, with
1533 the pilus only bringing the cells together by retracting with the recipient cell attached.

1534 Like in iDynoMiCS 1, plasmid carrying cells search the neighborhood within the reach of the pilus. A
1535 difference arises in the method implemented for this search. Instead of the “scan speed” in iDynoMiCS
1536 1, the required parameters are maximum pilus length and “transfer probability”. Using the F-pili data
1537 from live cell imaging by Clarke *et al.* (2008), the pilus length can be calculated for each time step of
1538 the process as a function of extension speed. The current length is used as the maximum distance for
1539 neighborhood search. The closest neighbors are prioritized by increasing the neighbor search range in
1540 increments of 0.01 μm until the current pilus length is reached or a neighbor is found. As an example,
1541 with pilus length of 3.2 μm , a neighborhood search will be performed 320 times with the distance
1542 searched increased from 0.01 to 3.2 in increments of 0.01 μm . The search will be terminated early if a
1543 plasmid-free neighbor is found.

1544 Once a plasmid free neighbor is found, the transfer event happens instantly with a success probability
1545 given by the parameter “transfer probability”. Biologically, the transfer happens after pilus retraction
1546 and then the plasmid goes into a “cool down” period. To reduce the computational requirement for
1547 agent movements, the time for retraction of the longest pilus is added to the cool down period as a
1548 wait time between plasmid transfer attempts.

1549 **Table S13. Parameters required for the plasmid dynamics process manager in iDynoMiCS 2.0.**

Parameter	Definition
Transfer probability	Governs the success of plasmid transfer; user must provide either one of the parameters with the relation being: Transfer probability = frequency × number of neighbors
Transfer frequency	
Loss probability	Governs the success of loss event upon cell division
Pilus length	Maximum length of pilus extension from donor cell surface. If plasmid transfer is not pilus driven, this can be set to 0
Aspects to Transfer	Agent aspects to change on plasmid acquisition or loss (MIC, Fitness cost, etc.)
Cool down	Rest time between plasmid transfers
Extension speed	Extension speed for pilus related to this plasmid
Retraction speed	Retraction speed for pilus related to this plasmid. The time for complete retraction is added to the cool down time before the next transfer can start

1550 Since each plasmid is a separate aspect specified in the protocol file, there can be multiple plasmids
1551 included. These will implicitly be considered compatible with each other as plasmid incompatibility is
1552 not currently implemented.

1553 Plasmid loss due to segregation is defined as an event in the code, thus requiring inclusion as an aspect
1554 in the protocol file. However, the event is triggered upon cell division only if the “loss probability”
1555 parameter is defined in the included plasmid dynamics process manager. Thus, upon cell division, the
1556 daughter cells can retain the plasmid or one can lose it at the probability defined in the protocol file.

1557 For chemostats, the transfer process is governed by the following equation to determine the number
1558 of transfers for each agent with plasmid (donor):

1559
$$\frac{\beta R}{R + 1} \Delta t$$

1560 Where β is the transfer frequency, R is the number of plasmid-free agents (recipients) in the population
1561 and Δt is the time step size. This equation is calculated for each donor so implicitly, the rate is
1562 proportional to donor concentration. It is analogous to the infection rate in Susceptible-Infectious-
1563 Recovered compartmental epidemiological models, where recipients are considered Susceptible and
1564 plasmid transfer is analogous to the process of infection. The recipients for the plasmid are selected
1565 randomly from the whole population as a chemostat is considered well-mixed.

1566 S1.12 Agent density scaling for 2D simulations

1567 Due to the virtual third dimension of 1 μm in 2D simulations, cell radii and/or lengths can differ
1568 between 2D and 3D compartments. iDynoMiCS 2.0 can scale agent densities, such that the dimensions
1569 of agents in 2D match what they would be in a 3D environment.

1570 Users define an actual 3D density, ρ_{3D} , which is then used to calculate a scaled density in the 2D
1571 compartment, ρ_{2D} . The exact calculation depends on the shape of the agent or filament section in
1572 question.

1573 For spherical (coccoïd) agents, the radius of a sphere is calculated based on the agent's mass and actual
1574 density:

$$1575 \quad r_c = \sqrt[3]{\frac{3}{4\pi} \frac{m}{\rho_{3D}}}$$

1576 Where r_c is the radius and m the agent's total mass. The scaled density is thus given by:

$$1577 \quad \rho_{2D} = \frac{m}{\pi r_c^2}$$

1578 For agents or filament elements with a rod (bacillus) shape, it is the length, rather than the radius, that
1579 must be calculated. The 3D length of the line-segment connecting the agent's points is given by:

$$1580 \quad l = \left(\frac{m}{\rho_{3D}} - \frac{4}{3} \pi r_c^3 \right) / \pi r_c^2$$

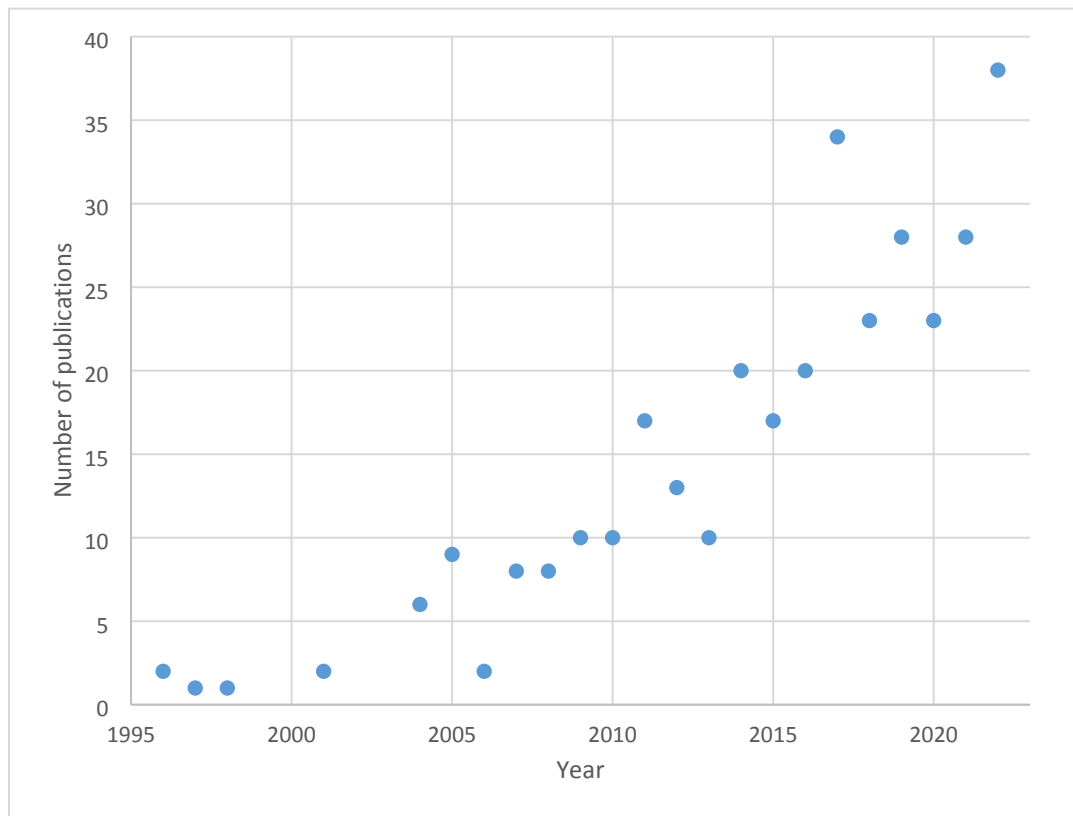
1581 And the 2D scaled density is given by:

$$1582 \quad \rho_{2D} = m / (\pi r_c^2 + 2r_c l)$$

1583

1584 S1.13 Microbial IbM publications on PubMed

1585



1586

1587 **Fig S9. The number of publications on microbial IbM on PubMed since 1995.** A simple search query
1588 on PubMed reveals a growing trend in applying IbM to microorganisms. The following query was used:
1589 “((biofilm) OR (microbial)) AND ((individual-based) OR (agent-based)) AND (model)”.